

A REVIEW OF ICE LOADING AND THE EVOLUTION OF THE FINNISH-SWEDISH ICE CLASS RULES

Kaj Riska, DSc.
Director, Helsinki, ILS Oy
Professor, Norwegian University for Science and Technology

Jorma Kämäräinen, DSc.
Senior Maritime Inspector, Finnish Transport Safety Agency

DRAFT TO THE SNAME ANNUAL MEETING IN 2011

ABSTRACT

The Finnish-Swedish Ice Class Rules (FSICR) have their origin in rules given in 1890. Since that time, the rules have evolved and, at present, the FSICR can be considered an ‘industry standard’ for designing ships for first-year ice environments. The evolution of the rules has mostly been based on feedback from ships, in the form of ice damage, though new research results have also influenced rule development. In this article, the background to the hull rules in the FSICR is described and analyzed. First, it makes it clear that the rules are an integral part of the winter navigation system for Finland and Sweden. The rule formulations are described and great attention is given to analyzing the design point in the rules – the design point includes the limit state used and the frequency of reaching it. In order to analyze the design point, statistics of ice loads are investigated, based mainly on the measurements carried out in the Baltic. The analysis of the design point in the FSICR suggests that it entails reaching the yield limit once in a winter or the plastic limit once in a ship’s lifetime. The strength of the plating and frames is also quite balanced.

Keywords: Icebreaker, ice load, ice rules, ice load measurements, plastic response

1. INTRODUCTION

Navigation in ice-covered waters used to be a seasonal adventure during the sailing ship era. With sail powered ships, ice could not be broken, only avoided. With the advent of steel hulls, power by steam, and, later, diesel engines and propulsion by propellers, ice could be forced to a certain extent. The first real winter navigation started in the Great Lakes in the mid-19th century. It quickly became evident that more economical and safe navigation would be achieved if special purpose icebreakers were used to assist the less ice-capable merchant ships. The first steam-powered icebreaking ship was the **City Ice Boat No. 1**, built by the city of Philadelphia in 1837. She was a wooden paddle steamer intended to break ice in the harbor. The first European steam-powered icebreaker, as well as the first ever metal-hull icebreaker, was the Russian **Pilot**, built in 1864. Its bow had been designed with some ice-breaking capability (the stem angle was 20°). These and other early icebreakers were able to extend the summer season, but it took several decades, to the end of the 19th century, before navigation through ice – winter navigation – started to have economical importance.

When winter navigation commenced on an economically significant scale, it became necessary to regulate the construction and use of ships intended for ice. The first rules for winter navigation were issued in Finland in 1890 – these were called the Imperial Statutes for construction and fitting out ships for winter navigation (see, e.g., Siivonen 1977), as Finland was part of Russia at that time. Since that time, many updates to the Finnish ice class rules have been made: updates that have been necessary in view of the feedback from the earlier rules in the form of data about ice damage, or

when new technical solutions have been introduced. The Finnish ice class rules have and still are an example for classification societies and, at present, these rules can be considered an industry standard for ships navigating in sea areas in which there is only first-year ice.

Each set of Finnish ice class rules (since 1932, there have been more than one strengthening level, ice class, in the ice class rules) is based on some idea about ice loading as well as some acceptable strength level. As knowledge about ice loads improves and feedback from ice damage accumulates, changes to the rule foundation warrant rule updates. In this paper, the knowledge background that forms the foundation for the present Finnish-Swedish Ice Class Rules (FSICR) is described. The aim is to make the rule background transparent and indicate how the new knowledge could be incorporated into the rule updates. The FSICR include requirements for hull and machinery scantlings as well as for the minimum propulsion power of ships, but the present article is restricted to describing only the hull rules.

The aim of the article is to describe the design point of the hull structures in the FSICR. The design point includes a description of the loading, especially frequency and magnitude, and allowable response. As the FSICR are an integrated part of Baltic winter navigation, the background to the FSICR is described first. After this, the rules themselves are described in short, followed by a lengthy description of the factors included in determining the rule ice loading. The structural response to be included in the design point is described before the design point that is finally selected (and some alternatives to it) is touched upon. The article tries to show that putting together ice class rules is a holistic process in which many different parts of the rules interact. Thus, it is not possible just to change one part of the rules that is deemed incorrect without a complete revision or at least a review.

2. BACKGROUND TO THE FINNISH-SWEDISH ICE CLASS RULES

Finland is one of two countries in the world whose ports are all ice bound every (average) winter – Estonia being the other. Fluent, efficient, and economical winter navigation is thus a prerequisite of all economic activity in Finland. Even Sweden is less dependent on winter navigation, as ports south of Stockholm only experience minor hindrance from ice.

2.1 Winter Navigation System

The Finnish and Swedish winter navigation system is based on: a) icebreakers that escort the merchant fleet through the worst ice conditions; b) an ice-strengthened merchant fleet; and c) actions of maritime authorities (rules, regulations, and fees). As the Baltic has seasonal ice cover, the ice season lasts from three to five months annually, and all Finnish ports are icebound every average winter, ships visiting Finland and northern Sweden year-round must be ice capable. The merchant ships sailing in the northern Baltic compete with open water ships during a large part of the year, thus the ice strengthening and ice performance must not have a great effect on their competitiveness, vis-à-vis the open water ships. This has led to the present balance between the required ice capability of merchant ships and the number of icebreakers escorting them, and the safety level of winter navigation. The interaction between the different parts of winter navigation makes it a system. The interacting parts of the Finnish winter navigation system are shown in Fig. 1.

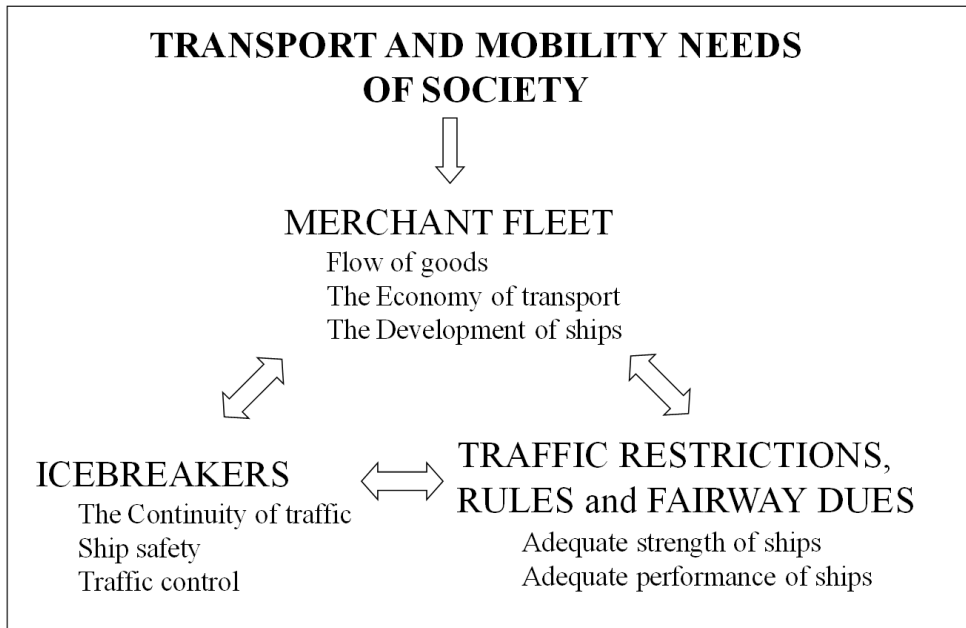


Fig. 1. Interacting parts of the Finnish winter navigation system

2.2 Elements of the Winter Navigation System

The maritime authorities set the FSICR and the requirements for ice classes (traffic restrictions) as well as the fairway dues. The Finnish-Swedish Ice Class Rules include requirements for the ship hull and machinery strength as well as some requirement for ship performance in ice. The requirement for ice performance interacts with the icebreaker escort service: if the merchant ships had lower ice performance, they would need more icebreaker escorts. More icebreakers would then be needed to serve all the ships – as all ships fulfilling the traffic restrictions are given icebreaker escort, if needed – and this would lead to increased costs. The increased costs would be covered by higher fairway dues. The Finnish fairway dues are scaled with the ice class: higher ice class ships pay lower fairway dues. The Finnish winter ports and the average extent of ice cover in the Baltic are shown in Fig. 2.



Fig. 2. Average extent of ice cover (white area outside the ports) in the Baltic and Finnish winter ports (red dots) (www.liikennevirasto.fi)

In order to reduce the escort times of merchant ships and to make winter navigation as efficient as possible, requirements are set for ice classes and for a minimum amount of cargo. These restrictions are set for each port and are increased as the winter progresses, following the development of the ice cover. The rationale of the minimum amount of cargo is that if each ship only carries a small amount of cargo, more ships are needed for a certain amount of trade and thus more icebreaker escorts are required per transported ton. The traffic restrictions are declared roughly one week before they come into force, and they are published on the home page of the Finnish Transport Agency (www.liikennevirasto.fi). The traffic restrictions are also shown in the daily ice charts issued by the Finnish (and at the same time Swedish) Ice Service; see Fig. 3. The ice charts contain information about the ice cover, traffic restrictions, and icebreakers active in different sea areas.

The fairway dues are scaled according to the ice class, and the amount of the fairway due is set by the net tonnage (NT) of each ship. There is a maximum amount of fairway due (at present 98,400 €). The fairway due is paid for each port visit, though cargo ships do not need to pay the fairway due more than 10 times per year (30 times per year for passenger ships). The amount of the fairway dues for cargo ships is shown in Fig. 4. Passenger ships pay roughly two-thirds of the amount for cargo ships.

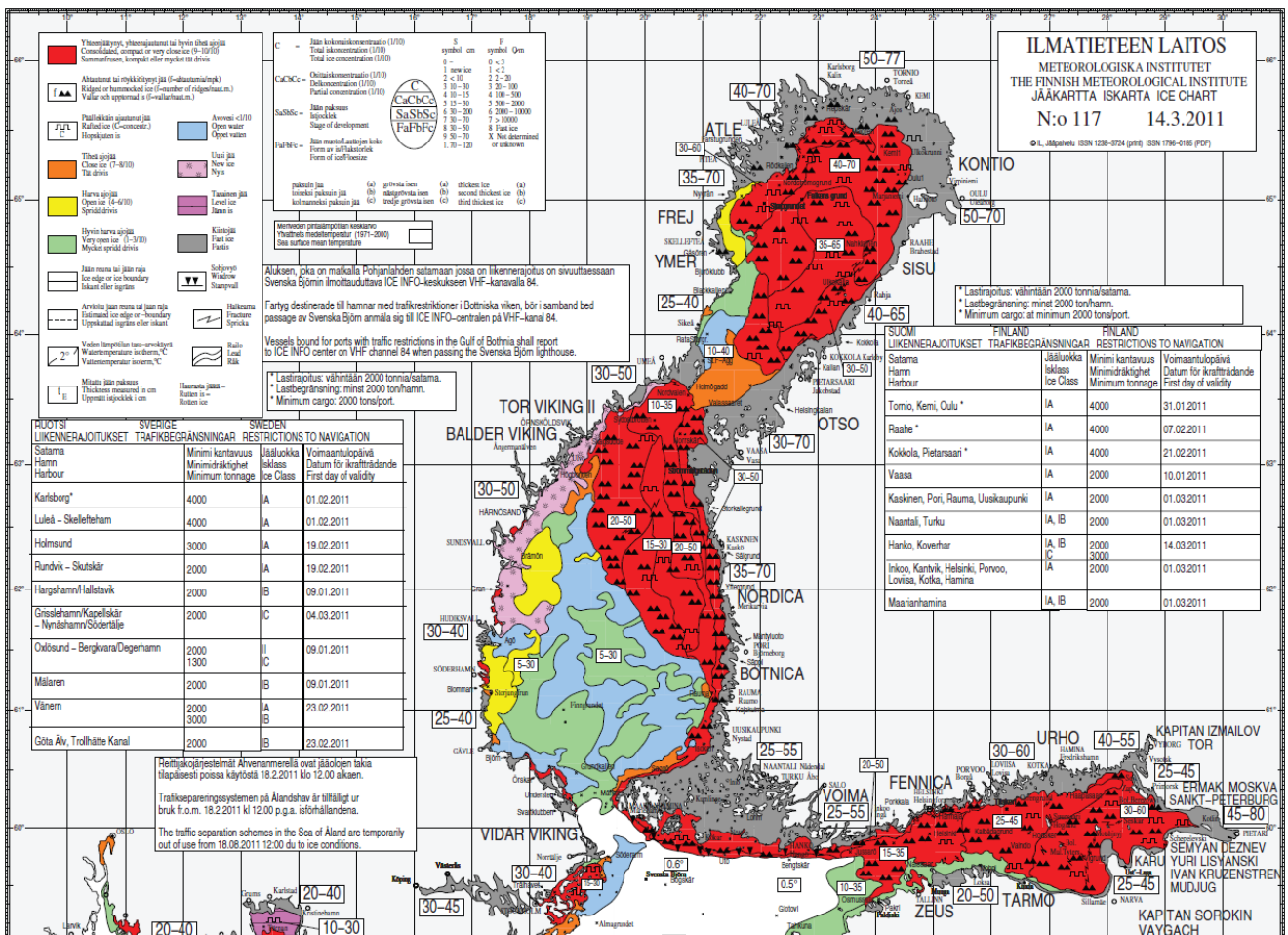


Fig. 3. Ice cover in the Baltic, Swedish and Finnish traffic restrictions (text boxes on the left and the right), and approximate icebreaker locations (the text in the figure is small and the original ice charts can be downloaded from www.fmi.fi)

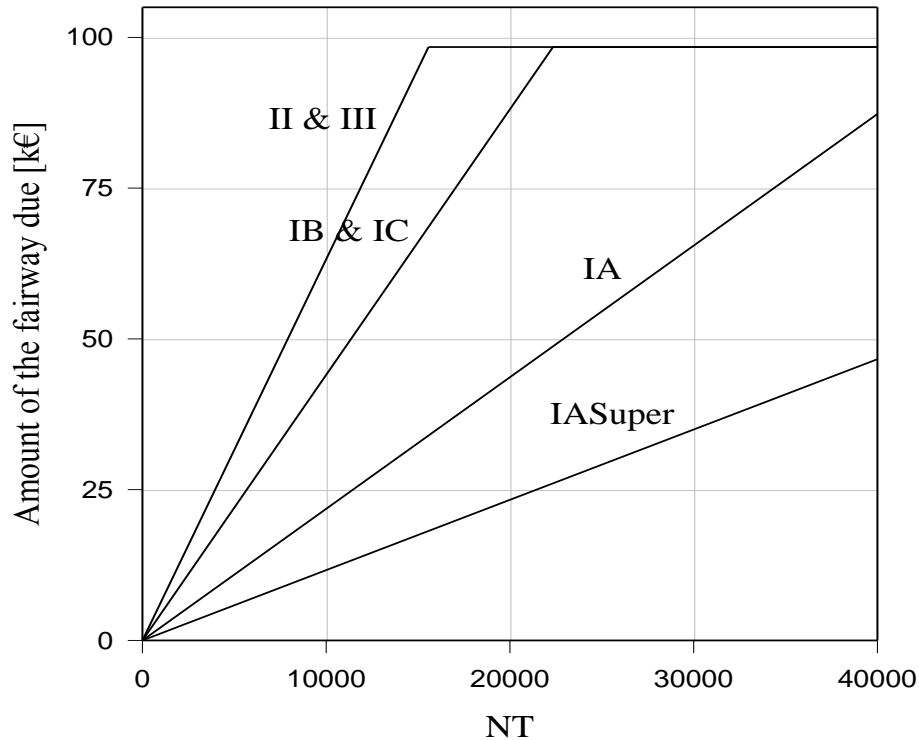


Fig. 4. Amount of fairway due per port visit in Finland for cargo ships (from 1/1/2009, Act 787/2008)

2.3 Evolution of the FSICR

The first Finnish rules for winter navigation were given in 1890. These rules only contained requirements for ship equipment (e.g., how many pairs of skates and skis had to be on board) and the general and structural arrangements on the ship. The first Finnish ice class rules for shipping were given in 1920. These rules started the long tradition of the so-called ‘percentage rules.’ In these rules, the scantlings were set as some relative increase in the open water scantlings. If the relative increase in the plate thickness and the frame section modulus are the same, the percentage practice leads to a greater increase in plate strength, as plate thickness is proportional to the square root of the strength, whereas the frame section modulus is linearly dependent on strength. This works against a sound structural strength hierarchy. The first Finnish ice class rules were given in 1932, when three ice classes (IA, IB, and IC) were introduced, as well as ice class II corresponding to open water ships and ice class III corresponding to barges. At this time, the ice classes were also coupled with the fairway dues. Only minor corrections to these rules have been made in four decades, and the last change was the introduction of ice class IA Super in 1965.

The year-round trade to northern Finnish ports (Kemi, Oulu, and Raahе, as well as the Swedish port of Luleå) increased greatly in the 1960s. The increased trade caused three major changes to the Finnish winter navigation system. The first one was that ships built according to the percentage rules were found to be too weak – in the sense that the amount of ice damage exceeded the economic pain threshold. This led to a large ice damage survey and complete revision of the ice class rules; see Johansson (1967). For the first time, the damage survey gave an idea of the magnitude of the ice pressure, with the cost of fixing the load height – this was chosen to be the same as the maximum level of ice thickness, i.e., 800 mm. The rules themselves, based on the ice damage survey, were published in 1971.

The second major change to the Finnish winter navigation system was a result of an agreement between Finland and Sweden to develop the winter navigation system together. Icebreaker services in the Bothnian Bay and Sea would also be organized together. As the ice class rules are an essential part of the winter navigation system, the rules were to be given jointly; thus the 1971 set of rules is called the Finnish-Swedish Ice Class Rules. The third major change to the winter navigation system was the realization that far more powerful icebreakers were needed. The result was the development of Urho class icebreakers, which have almost twice the power of the (at that time) previous icebreakers. The Urho class, delivered between 1974 and 1977, can be considered the last classic icebreaker class with two bow and two stern propellers.

The next revision of the FSICR occurred in 1985 when the hull rules were changed. The main change was to the ice load height, based on extensive ice load measurements on merchant ships and icebreakers; see for example, Vuorio et al. (1979), or Kujala and Vuorio (1986). The measurements showed that the load height compatible with the measured ice load **and** structural response is much less than the ice thickness. The ice load height was made the ice class factor instead of ice pressure. The idea here was that ice is similar, even if the thickness is somewhat greater, and thus the ice pressure, being an ice material constant, is the same for each ice class, but as the ice thickness related to each ice class is different, the load heights are consequently different for each ice class. While the load height changed, the line load determined from the ice damage data remained constant in the rules. This new idea of the ice load is indicated in Fig. 5.

A possible future scenario for the ice load height is presented in Fig. 5. Recent measurements indicate that the ice edge is failing in a fashion to create a very narrow contact between the structure and the ice edge. This produces a very small contact height; see, for example, the first observation of this type of contact in Riska et al. (1990). The problem, for design purposes, of this line-like contact is that while the local pressures are high (at least 60 MPa has been measured in a very small area; see Frederking and Sudom [2008]), the measured ice load obtained from controlled tests divided by the load length along the contact line, q , is relatively small compared with the measured values from ship tests. It has also been observed that when ice is relatively warm (close to melting point) or the relative velocity between the ice edge and structure is low (some cm/s), the ice does not fail in a manner that produces the line but rather so that the contact is on the whole height of the ice sheet. At the same time, the line load q is larger than in the brittle case, in which the line forms; see Sodhi et al. (1998). The design case is not clear, but the suggestions for future research given toward the end of the paper have now already been anticipated.

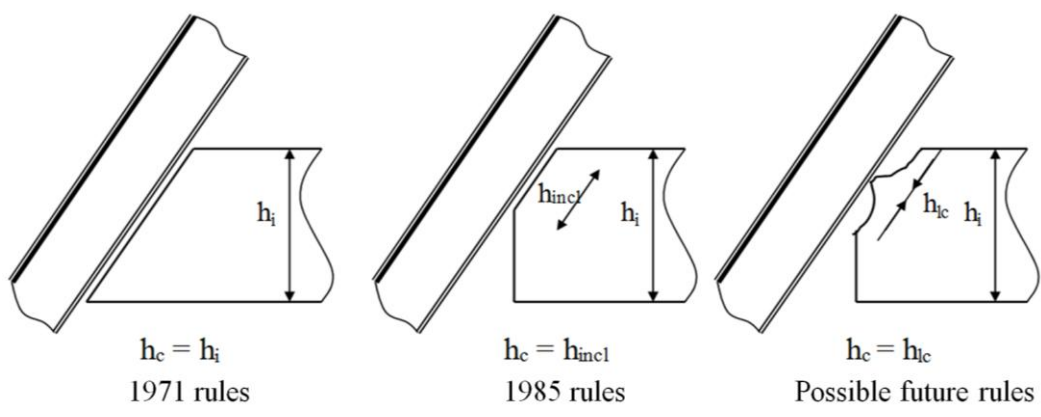


Fig. 5. Sketch of the concept of load height on a ship frame with different rule sets. In all these cases, the value of the line load q has been constant, at about $q = 2 \text{ MN/m}$.

The 1932 ice class rules already contained a requirement for performance in ice – this was given as the required propulsion power (P_D) as a function of the product of ship length and breadth (this

product was changed to displacement in the 1971 rules), with different constants for each ice class. In the 1985 rules, this power requirement was amended so that the constants in the previous equation included some dependency on ship beam and bow shape. The ice performance requirement was changed drastically in 1999 (and slightly amended in 2002) when an ice performance requirement (instead of power requirement) was introduced. The requirement states that the ship must be able to maintain a speed of at least 5 knots in a brash ice channel the thickness of which is a class factor (1 m for the ice class IA). If the designer cannot show compliance with this, the rules give an equation for the rule channel resistance (R_{CH}) and propulsion power. The 1999 rules give quite high propulsion power for large ships, see Fig. 6, and thus the rules contain a proviso for this kind of case. In fact, the rules state that the designer can show compliance with the ice performance requirement by, e.g., conducting ice model tests. This has led to quite low levels of propulsion power for ships. Results of ice model tests and full-scale tests, P_{Dmeas} and R_{CHmeas} , normalized by the required ice class power (P_{Dreq}) or rule ice resistance (R_{CHreq}) are shown in Fig. 6. The full-scale power values straddle the rule requirements well. All the test results shown in Fig. 6 have been amended to correct the channel thickness.

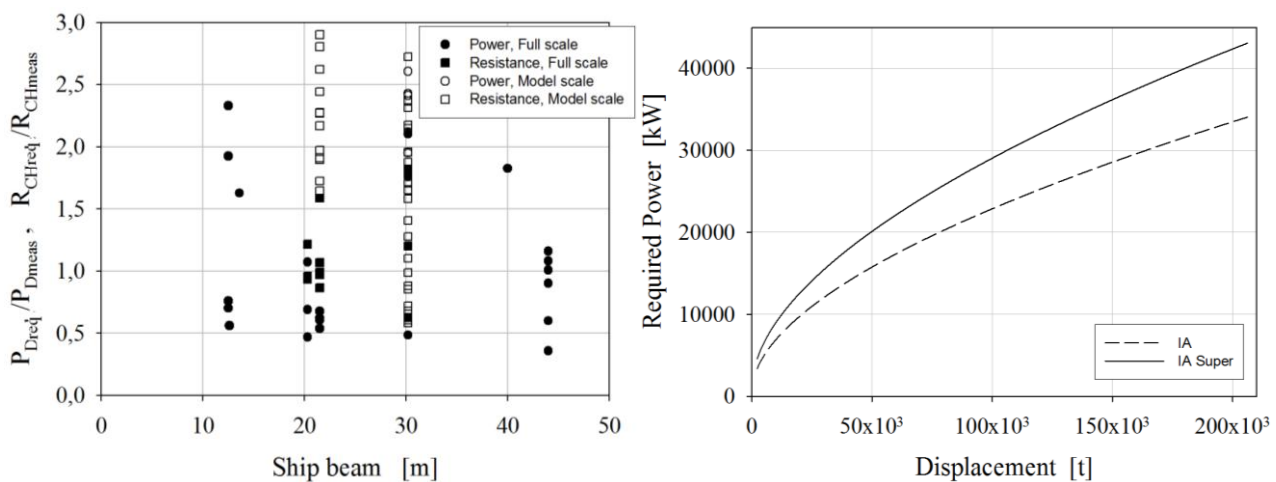


Fig. 6. Some observed cases of propulsion power and channel resistance from ice model tests and full-scale tests in which the channel thickness is known (left) and the required propulsion power for AFRAMAX-shaped ships of various sizes (Riska 2006a, b)

The FSICR were further updated with regard to the ice water lines (2006): the ship draught must be between the Upper and Lower Ice Water Line (UIWL and LIWL) when operating in ice. These waterlines may deviate from the ones given in the draught mark. In 2008, the new machinery rules were introduced. This time, the whole structure of the machinery rules was changed. Since the 1971 rules, the machinery rules have been based on the concept of ice torque $Q = m \cdot D_P^2$ where m is a class factor and D_P the propeller diameter. The new rules only give the ice loads on the propeller and the designer must calculate the propeller scantlings himself/herself.

The most recent change in the FSICR has been to streamline the hull rules. This was done in 2010. When the rules were updated in 1985, several factors were introduced, the background to which is somewhat obscure. The aim in 1985 was not to change the strength level for transverse frames (the new idea of load height had a large impact on longitudinally framed structures). These factors were now put into the context of the newer research results. These 2010 Finnish-Swedish Ice Class Rules form the basis of this paper, and the background to the hull rule formulation is described.

This short elaboration on the evolution of the Finnish-Swedish Ice Class Rules shows that the strength level included in the rules is under constant scrutiny – this scrutiny is provided by the approximately 12,000 ship visits to Finnish ports every winter. Ice damage surveys like the one by

Hänninen (2005) suggest that some damage occurs to ship hulls, propellers, and rudders every winter. This indicates that the strength level is not set too high, and as the amount of damage is small it can be considered as not being too low either. This validation of the FSICR every winter since the present strength level was first introduced for transverse frames (other parts have been updated) in 1971 makes the Finnish-Swedish Ice Class Rules very robust and reliable.

3. STRUCTURE OF FINNISH-SWEDISH ICE CLASS RULES

Four ice classes are defined in the Finnish-Swedish Ice Class Rules. These are in order of strength from high to low: IA Super, IA, IB, and IC. The strength level in each ice class corresponds roughly to the loading from a certain level of ice thickness: for IA Super 1.0 m down to IC 0.4 m. The ice thickness for IA Super is higher than the maximum level of ice thickness observed in the Baltic outside the fast ice zone. The design point for each ice class is a collision with a channel edge (as ships are escorted in the worst ice conditions) or with a consolidated layer of older ridges. As the consolidated layer of ridges may be 1.8 times thicker than the level ice at the same location, and the maximum average level ice thickness in the middle of the sea basins is about 60 cm, this results in about 1.0-m-thick ice. It should be noted that this design scenario does not state ship speed – it is considered that no speed restrictions should exist, as this would handicap much of the navigation in ice. It is still somewhat unclear, however, which ship-ice interaction scenario causes the highest loads. This uncertainty in the design scenario is discussed briefly in Section 4.5.

The Finnish-Swedish Ice Class Rules (TRAFI 2010) consist of three main parts: rules for the performance of ships in ice, rules for hull strength, and rules for machinery strength. There are also regulations for ice class draught, rudder and steering arrangements, and some miscellaneous machinery requirements. The topic in this paper is the regulations concerning hull strength, and the quantities included in the hull rules are now described.

3.1 Ice Pressure and Ice Load

The definition of the ice load is the most important part of the hull rules. The ice load in the FSICR is, in principle, defined so that the ice pressure is constant for all classes (nominal ice pressure p_0) and the load height h is the class factor (from 0.35 m for ice class IA Super to 0.22 m for ice class IC). The magnitude of the nominal ice pressure is 5.6 MPa. This approach of constant pressure is taken as the material properties of the Baltic ice do not change much through the winter in different Baltic Sea areas. The total ice load for each structural member is then taken as the line load

$$q = p \cdot h \tag{1}$$

times a load length l_a that depends on the width (horizontal span or spacing) of each structural member. For transverse frames the load is, for example, $F = q \cdot s$, where s is the frame spacing.

To obtain the ice pressure p , the nominal ice pressure is modified by three multiplicative coefficients, all of which are less than one. The ice damage study carried out in the late 1960s, which resulted in the 1971 rules, indicated that the ship size influences the ice load. An analysis of the mechanics of collision between ice and a ship suggests that it is the ship displacement and speed that influence the contact force. The total contact force in collisions with ice is not an important factor for most of the structural members (they are sensitive to a load patch that is smaller than the total load patch size) however. This has led to the definition of the size quantity of

$$k = \sqrt{P \cdot \Delta} \tag{2}$$

and a size coefficient for ice pressure c_d , which is linearly dependent on k . The value of k for a typical Baltic ship ($P = 4$ MW, $\Delta = 15000$ t) is $k = 7.7$ and the size coefficient $c_d = 0.46$ (bow region).

The ship hull is divided into the three hull regions shown in Fig. 7: bow, midbody, and stern. Each of these has a design ice pressure defined by a hull region factor c_p . This factor is for the bow region and is scaled according to the ice class for other regions so that the stern region has the lowest design ice pressure. For ice class IC, the stern hull region coefficient is 0.25.

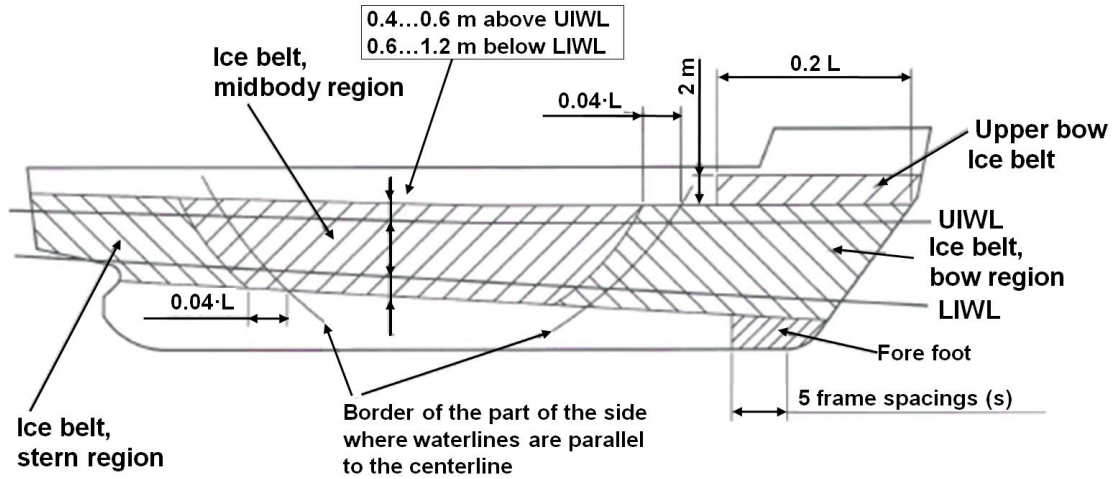


Fig. 7. The hull regions defined in the FSICR

The third factor used to define the ice pressure is a coefficient dependent on the load length, c_a . Each structural member has an associated load length l_a – this is the length of the load that influences the response (stress) in the member. The load length coefficient is defined as

$$c_a = \sqrt{\frac{l_0}{l_a}}, \text{ max } 1.0 \text{ and min } 0.35 \quad (3)$$

where the reference length is $l_0 = 0.6$ m. In principle, each structural member should be designed by trying all load lengths and then selecting the design case to be the length that gives the maximum stress. There is no need to do this calculation, as the load lengths are given in the rules, as shown in Table 1.

Table 1. Load lengths associated with different structural members

Structural member	Type of framing	Design load length l_a [m]
Shell plating	Transverse	Frame spacing
	Longitudinal	$1.7 \cdot$ frame spacing
Frames	Transverse	Frame spacing
	Longitudinal	Span of frame
Ice stringer		Span of stringer
Web frame		$2 \cdot$ web frame spacing

The design ice pressure is finally

$$p = c_d \cdot c_p \cdot c_a \cdot p_0. \quad (4)$$

Even if the design ice pressure at the bow region is the same for a ship in all ice classes, the design force is not, as the load height is a class factor.

3.2 Scantlings

Once the ice load is specified and the limit state is defined, the scantlings can be calculated. The limit state used in the Finnish-Swedish Ice Class Rules is the yield limit – consequently, only the elastic response of the structures needs to be derived. The plate thickness equations are based on a similar equation used to design car decks under tire loading. The frame equations are based on simple beam formulation. The effect of load height on plate response is taken into account with a constant dependent on h/s (the constant is denoted here as $f(h/s)$) – plate thickness t is given by equations of the form

$$t = \frac{2}{3} s \cdot \sqrt{f(h/s) \cdot \frac{p_{PL}}{\sigma_y}}, \quad (5)$$

where p_{PL} is the equivalent plate pressure, at $0.75p$, and σ_y is the yield strength. The origin of the constant 0.75 is in the pressure distribution across the plate and is discussed in Section 4.4. The constant $f(h/s)$ is different for transversely and longitudinally framed structures.

The frame scantlings include the frame section modulus Z and shear area A . These are calculated for transverse frames with equations of the form

$$\begin{aligned} Z &= \frac{q \cdot s \cdot l_a}{m \cdot \sigma_y} \\ A &= \frac{1}{2} \cdot \frac{1.2 \cdot q \cdot l_a}{\tau_y} \end{aligned} \quad (6)$$

where τ_y is the shear strength and the factor 1.2 stems from taking the shear stress distribution across the web into account. m is a factor dependent on the end connections of the frame ($m = 5 \dots 7$). The equations for longitudinal frames are similar but contain a factor that is dependent on the load height and frame spacing.

The structure of the hull rules is presented schematically in Fig. 8.

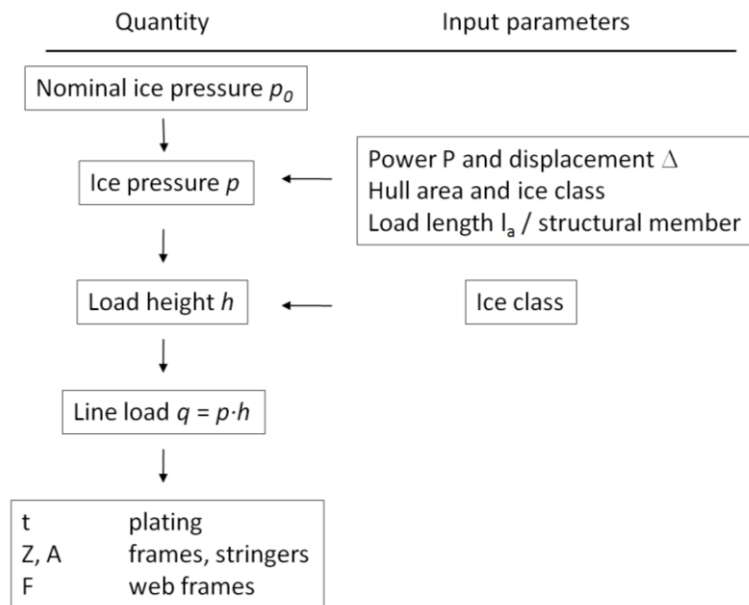


Fig. 8. The structure of the hull rules in FSICR

3.3 Some Observations

The structure of the Finnish-Swedish Ice Class Rules is quite simple and the flow of the calculations is easy to follow and perform. Some observations can be made, however, concerning the structure of the rules and the main points of the rule rationale. These observations include:

- a) The ice load is independent of the hull shape. The simplicity of the formulation is the main reason for this, and not much knowledge exists on the effect of the hull shape. The load is constant along the whole bow and can be qualitatively justified by the fact that two physical effects influence the load: speed of indentation into the ice and frame angle. The indentation speed depends on the projection of speed on the shell normal. This decreases when moving from the stem towards the bow shoulder area. The frame normal angle (frame inclination on the vertical plane including the frame normal) is usually greatest at the bow and decreases towards the shoulder area. The ice load increases with the indentation speed, whereas the load decreases with the frame normal angle – these effects have opposite trends along the bow waterline.
- b) According to some other ice class rules, the longitudinal location of the structures influences the required scantlings. This is not the case in the FSICR and similar argumentation as that used above.
- c) The ship size description includes both the power and displacement through the factor k . This factor could be called an ‘aggressiveness factor’ as it describes the ship inertia and instantaneous speed. The drawback is that there is no theoretical justification for the use of this factor. This question is investigated briefly in Section 4.2.
- d) The design point includes the yield as the limit state. If the loading for plating and framing had similar return periods (see Chapter 6), this would induce an unsafe structural strength hierarchy. Plating and frames would be of similar strength and, as frames have less plastic reserve than plating, under ultimate loads the frames would collapse, first leading to greater damage than just plating failing. This is corrected in the present rules, however, with different safety factors for plating and frames.

Now that the structure of the Finnish-Swedish Ice Class Rules is clear, it is time to turn to the background of these hull rules. Here, only the most important elements of the background are described. The aim is to expose the knowledge basis for the different formulations that have been incorporated into the rules.

4. DESCRIPTION OF ICE LOAD

The ice load description is the core of any hull design for ice. The principles of the local ice load description in the Finnish-Swedish Ice Class Rules were described in Chapter 3 and a sketch of these was shown in Fig. 8. Here, the different aspects that have been included in the determination of rule loads are described with the aim of the rule structure becoming more transparent.

4.1 Ice Load Patch Quantities

For structural design purposes, the ice load is commonly assumed to be described by uniform ice pressure, termed p_{av} , on a rectangular load patch of height h and length l . Thus, the total force is $F = p_{av} \cdot h \cdot l$. The design ship-ice interaction in the Baltic is a collision with a level ice edge, a channel edge when the ship is escorted or with the consolidated layer of an ice ridge. In all these cases, the contact area, i.e., the load patch, is quite narrow in height: in other words, the aspect ratio of the load patch h/l is small. This load description suggests a useful load quantity mentioned already, that of the line load $q = p \cdot h$. The usefulness of the line load stems from the fact that many structural members are not sensitive to load height but rather to line load. Furthermore, the ice load measurements that are described in more depth in Section 4.5 give the ice load acting on one frame, which is $F = p \cdot h \cdot s = q \cdot s$ (assuming, of course, that the load length is more than one frame spacing s). Thus the line load q can be obtained directly from measurements. The other quantities from the ice load measurements to be used in this analysis are the frame stress on top of the frame flange σ_{FR} and the plate stress in the horizontal direction σ_{PL} .

The problem with the ice load is that it includes three quantities that are not well known individually. The only quantity that can be known with some confidence is the line load. This line load has been obtained directly from the full-scale measurements and by calculating the ice load from observed ice damage. The insight into the rule on ice load is made even more difficult as different structural members are not sensitive to the total load but to ice pressure (plating), line load (transverse frames), or line load along the whole span in the case of longitudinal frames. An investigation of the ship-ice interaction mechanics suggest that the total ice load F in a collision with ice is mostly dependent on the collision speed and ice thickness (or ice mass in the case of individual ice floes). The local ice pressure p is not dependent – at least not in the same way as the total force – on the ice thickness or collision speed. The indentation rate does influence the contact pressure but only below relatively low indentation rates (some cm/s). Here, the aim is not to discuss the various theories for ice loads or ice pressure but to look at what the rationale is for the rule ice load in the FSICR.

4.2 Ice Load Dependency on Ship Main Particulars

The ice pressure in the FSICR depends on the ship propulsion power and displacement through a factor k , which is given in Eq. (2). The power to be used in the calculation of the factor k is the actual power delivered continuously to the ship propellers (or propulsion). There has been some confusion concerning this actual power and the required rule power, but the situation is clear: the power to be used in calculations is the delivered power P_D . The factor k accounts for the possibility

of colliding with ice at high speed – thus the propulsion power – and the possibility of penetrating severe ice by using ship inertia. The latter scenario may occur in a channel in which there are thick side ridges, including a consolidated layer. A smaller vessel will not reach the side ridges as she is pushed back to the channel by ice, but a larger ship has a large inertia that will carry her to the consolidated layer of the side ridges.

The background to the quantity k is in the ice damage studies carried out in the late 1960s when the year-round navigation to all Finnish ports increased sharply. The ice damage study was carried out by calculating the strength of ship shell structures in the case of undamaged ships and estimating the ice load causing the observed damages (Johansson 1967). The calculation gave the line load accurately for transverse frames, but as the load height was assumed to be 800 mm, the ice pressure values deduced were low. A typical plot from the damage study is shown in Fig. 9. The points of damaged / undamaged ships were used to draw a line between these – this is also shown in Fig. 9. It is clear that the curve fit also uses some other insight than just the calculated points.

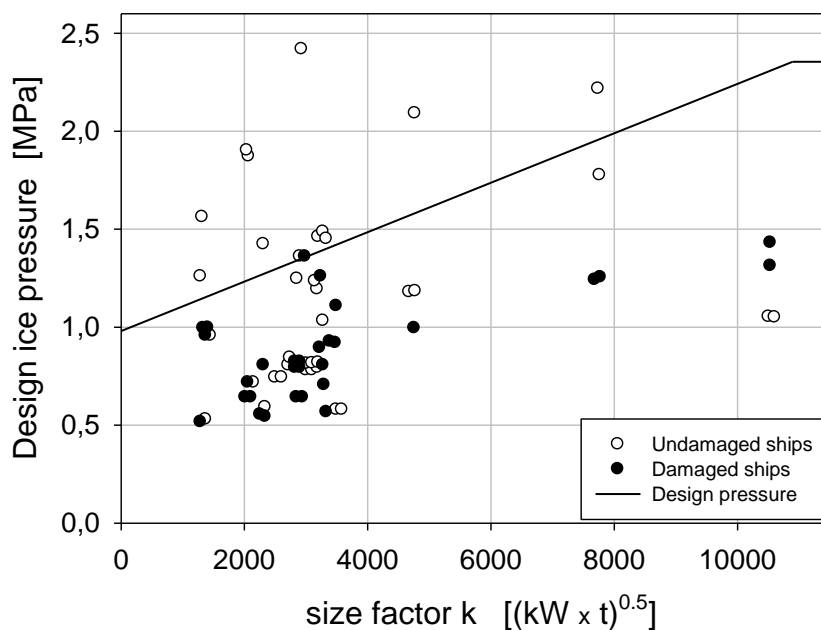


Fig. 9. Ice pressure causing the observed ice damage and the strength of undamaged ships for ice class IA ships at the bow (modified from Johansson 1967)

The rule ice pressure on the high and low ends of the ship size scale has been criticized: for the smaller vessels, the low end of the pressure – 1.29 MPa in the bow region – is considered low and the fact that there is no upper limit is considered unrealistic [this was corrected in the 2010 rules by introducing a ceiling]. At the high end, the bow ice pressure would exceed the nominal ice pressure $p_0 = 5.6$ MPa when $k = 80.3$. This corresponds roughly to a large SUEZMAX tanker of ice class IA Super ($\Delta = 170\,000$ dwt, $P_D = 30$ MW).

In order to investigate the size dependency of ice pressure, ice damage data from 2003 (Hänninen 2005) is analyzed. This is the last comprehensive survey of ice damage, a survey that includes ships built according to the 1985 rules. Fig. 10 shows the results of the ice damage survey carried out during winter 2003. The relative abundance of ice damage on different sizes of ships must be balanced with the relative number of this size of ship in traffic. Small ships (less than 2000 dwt) and large ships (more than 20,000 dwt) seem to be more susceptible to ice damage, as their total share of ice damage is 48%. Their share of ship traffic is only 19% however. The percentage of ships with

hull damage in different ship size categories is as follows, according to the data in Fig. 10 (27 cases of hull damage, about 863 ships in total):

> 20,000 dwt	12.3%
10,000-20,000 dwt	2.6%
4000-10,000 dwt	1.7%
2000-4000 dwt	2.2%
< 2000 dwt	6.7%

Damaged ships (hull damage)

Ship visits in winter 2003

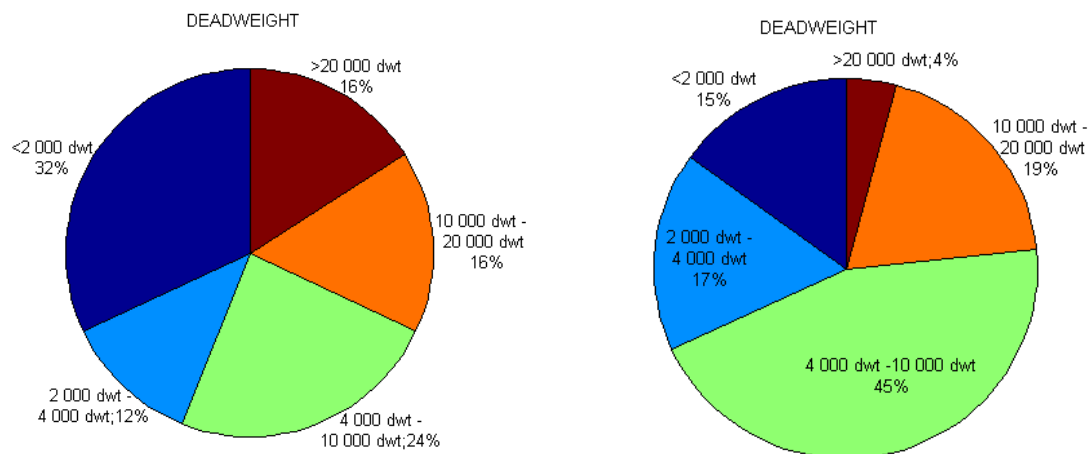


Fig. 10. Relative amount of hull ice damage during winter 2003 and relative number of ships visiting the Finnish ports during the same period (Hänninen 2005)

These figures suggest that there is a slight increase in the tendency for larger vessels to be less susceptible to ice damage, but the accuracy is not high in view of the small amount of ice damage to larger ships. Before a definite conclusion can be drawn from the damage data, the ships that have no ice class or were damaged below the ice belt should be removed from the statistics. This gives the results shown in Table 2. Even these data seem to show some bias towards the smaller end of the ship size, as two of the four damaged smaller vessels, measured with dwt, are actually quite large ships, passenger car ferries with a small deadweight. Thus, the small relative increase in the amount of damage in the small ship category is misleading, as half of the ships with a small dwt are actually quite large ships, similar in displacement to bulk carriers of about 6 ... 10,000 dwt. The larger ships seem to suffer slightly more ice damage.

Table 2. The relative and weighted amounts of ice damage for different sizes of ships

Ship dwt	Relative amount of all hull ice damage	Number of damaged ships in each size category
< 2000	30.8%	3.1%
2000-4000	0	0
4000-10 000	38.5%	1.3%
10 000-20 000	15.4%	1.2%
> 20 000	15.4%	5.8%

The dwt is not a good measure of ship size. Thus, a similar analysis of the ice damage frequency should be carried out for the modified data using the factor k . There is no distribution of ships visiting Finnish ports divided according to the factor k however. Thus, only the relative number of damaged ships can be given; see Table 3. As the average value of the factor k can be roughly

estimated from the fleet, giving a value of about 7, it can be concluded that there seems to be no trend in the dependency on the factor k .

Table 3. Relative and weighted amounts of ice damage in all ice damaged vessels in the survey for different sizes of ships

$k = \frac{\sqrt{P \cdot \Delta}}{1000}$	Relative amount of all hull ice damages
0-5	23.1%
5-10	46.2%
10-15	0
15-20	15.4%
20-25	0
25-30	7.7%
30-35	7.7%

It is also possible to look for the size dependency in the data from the ice load measurements. There are data from long-term (measurements covering at least one whole winter), full-scale ice load measurements in the Baltic from four ships: **IB Sisu**, **MT Kemira**, **MS Arcturus**, and **MT Kashira**. A collection of the data from these ships was made by Hänninen (2002). **MT Kemira** is described in Section 4.5 and, for the purpose here, it suffices to describe the other ships briefly. **IB Sisu** is a 16.8 MW icebreaker operating in the northern Baltic. The measurements were taken in winters from 1979 to 1985. **MS Arcturus** is a roro ship operating between Central Europe and the Gulf of Finland. Her ice class is IA Super. Three winters were covered in the local hull ice load measurements: 1985, 1986, and 1988. **MT Kashira** is a tanker operating in the Gulf of Finland and the Arctic (only Baltic measurements are considered here). Her ice class is UL, corresponding roughly to IA Super. The measurement years were 1985-1990. In this context, the frame ice load measurement results are investigated. These are collected in Table 4. The ships are arranged in order of severity of the ice conditions encountered (**IB Sisu** at the top). Furthermore, the ice load values given include the measured maximum and predicted most probable value in 1000 days. Taking into account the different areas of operation, no trend vs. k in the measured or predicted maxima can be discerned.

Table 4. The measured and predicted most probable (1000 days return period) frame ice line load values compared with the value of the size factor k .

Ship	k	Measured maximum [kN/m]	Predicted maximum [kN/m]
IB Sisu	12.5	1920	2290
MT Kemira	5.8	1850	2310
MV Arcturus	12.6	1350	2010
MT Kashira	6.7	1290	1780

The conclusion from the analysis of the size effect is that there is no strong suggestion to make changes to the present rule formulation. The only suggestion that can be made at this time is that a ceiling on the ice pressure is introduced. It is not likely that the frame ice load would increase

beyond the measured maximum of both IB **Sisu** and MT **Kemira**, i.e., about 2000 kN/m. With a maximum rule load height of 35 cm, this means that the maximum pressure could be set as the nominal ice pressure $p_0 = 5.6$ MPa. This decision is also justified by the fact that ships with a very large k factor value are large tankers (or bulkers) and are thus not likely to navigate in ice for as long or as aggressively as IB **Sisu** or MT **Kemira**.

4.3 Load Length Dependency

The ice pressure in the rule formulation depends on the load length. This is taken into account in the 2010 FSICR with a coefficient c_a given in Eq. (3), but it is repeated here for clarity

$$c_a = \sqrt{\frac{l_0}{l_a}}, \text{ max } 1.0 \text{ and min } 0.35; l_0 = 0.6 \text{ m.} \quad (7)$$

This coefficient is stated in the rules to account for “the probability that the full length of the area under consideration will be under pressure at the same time.” It greatly resembles the dependency of the average ice pressure on the load area, the formulation of which is used in offshore applications in particular – but for ships in first year ice, the load is more line-like and thus the dependency on the load length is used rather than the dependency on area. As the upper limit of the coefficient c_a is set to be reached with length $l_0 = 0.6$ m, it is clear that the coefficient is only important for longitudinal framing systems. As explained in Section 3.1 and shown in Table 1, each structural member has an associated load length. The plate response in longitudinal framing systems is sensitive to load length only up to a length of roughly twice the frame spacing (roughly the distance s from the point under study). Thus, the length used with the plating design in longitudinally framed structures is $l_0 = 1.7s$.

The present form of the length-related coefficient is based on a set of measurements from ships in the Arctic and the Baltic (see Frederking & Kubat 2005 for icebreakers **Louis S. St. Laurent**, **Oden**, and **Polar Sea**; Kujala and Vuorio [1986] for icebreaker **Sisu**; Kujala [1991] for ice damage data). All these data include simultaneous measurements (except, of course, the data based on ice damage data) of ice load on different lengths. The measured data are converted into a normalized line load in the form of

$$q = C \cdot l_a^x \quad (8)$$

by curve fitting. The values of the constant C and the exponent x are given in Table 5.

Table 5. Dependency of the line load value on the load length using the constants in Eq. (8)

	Louis S. St. Laurent	Oden	Polar Sea	Ice damage data	Sisu
C [MN/m ^{x+1}]	6.98	4.10	0.70	0.81	1.25
x	-0.60	-0.69	-0.60	-0.71	-0.54

There is an order of magnitude difference between the level of ice loading for **Louis S. St. Laurent** and **Oden** compared with the **Polar Sea** data, the Baltic ice damage data, and the **Sisu** data. Here, however, it is the form of the length dependency that matters. This form is given in Fig. 11. All the measured data follow a very similar form, and this form is thus taken as the basis for the new length dependency in the 2010 FSICR. To be slightly conservative, the exponent value of -0.5 was selected

for the rules. The cut-off at the length of 60 cm is somewhat arbitrary – it is set to correspond to roughly two transverse frame spacings.

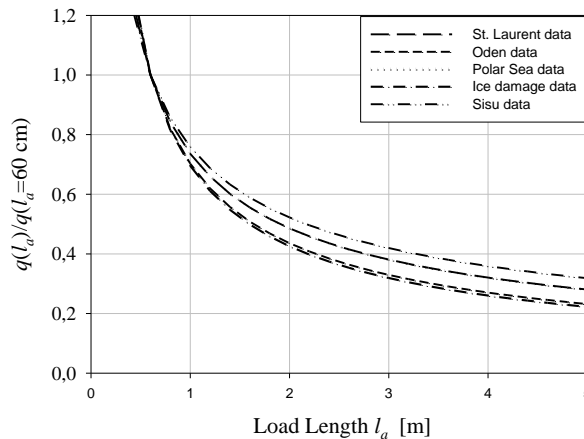


Fig. 11. Influence of the load length on the normalized line load obtained from measurements – the measurements are normalized with a load on a 60 cm length. The first three ships’ data are from Frederking and Kubat (2005), the fourth line from Kujala (1991), and the **Sisu** data from Kujala and Vuorio (1986).

4.4 Equivalent Ice Pressure for Plating

Ice load measurements in the Baltic have indicated that the maximum stress in a frame, the maximum stress at the adjacent plate field, and the ice force acting on the same frame are not compatible with each other if the ice pressure distribution is assumed uniform. It has been noted that especially the plate stress is lower than the calculated value using the measured ice load, assuming the ice pressure to be uniformly distributed (and a reasonable load height). This incompatibility has been associated with the flexibility of plating reducing the ice pressure in the middle of the frame span; see Vuorio et al. (1979). The phenomenon has been explained by the similarity with stiffened plating resting on an elastic foundation (Varsta 1983); if a framed structure is pressed against an elastic or Winkler (i.e., foundation sustaining only pressure, not shear forces) foundation, the contact pressure varies so that the pressure is lowest at the mid-span between the frames. This analogy from elastic foundations may be valid for transversely framed structures for which the line-like load continues over several frame spaces. The application of this pressure distribution to longitudinal framed plating may not be as directly applicable; see Fig. 12.

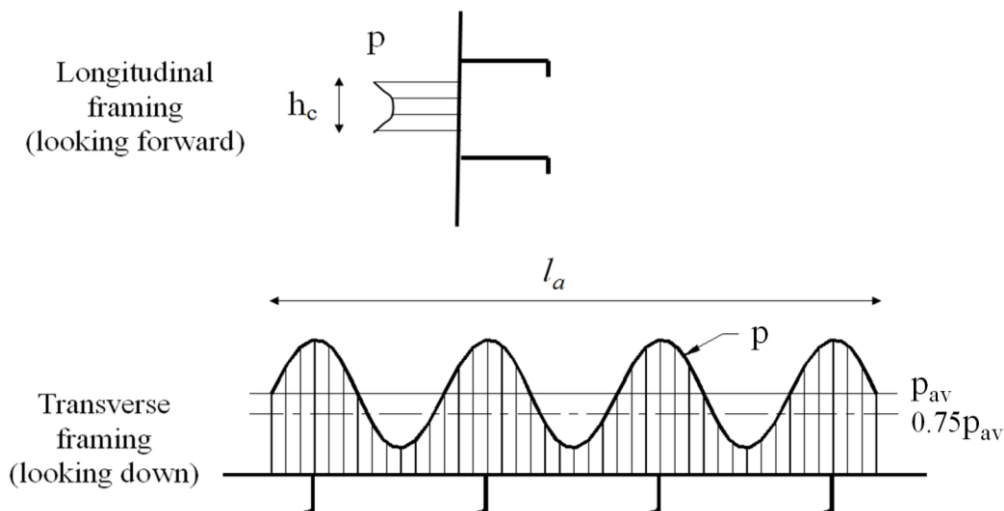


Fig. 12. Pressure distribution on longitudinally and transversely framed structures. p_{av} is the average ice pressure.

The effect of the pressure distribution on the response of transversely framed plating is taken into account in the ice class rules by introducing an effective plate ice pressure, which is

$$p_{PL} = 0.75 \cdot p. \quad (9)$$

The rationale behind this factor is that while the transverse frames are sensitive to the total frame load F , which is (x -coordinate defined in an obvious way and taking the pressure as constant in the vertical direction)

$$F = p_{av} \cdot h \cdot s = \int_0^s p(x) dx \cdot h, \quad (10)$$

the plating is also sensitive to the pressure shape, especially as the drop in pressure is at the mid-span. Thus, an equivalent ice pressure is defined as the average uniform pressure that gives the same maximum plate stress as the actual non-uniform pressure. In the FSICR, the equivalent ice pressure is taken as $0.75p$, where p is the rule frame pressure.

The plate flexibility depends on the plate thickness t and frame spacing s , and the pressure distribution has been shown (see Riska & Windeler 1997, Riska et al. 2002) to depend on the ‘flexibility length,’ which is given as

$$A = 4 \sqrt{k_f \cdot \frac{3(1-\nu^2)}{E \cdot t^3}}, \quad (11)$$

where ν and E are the Poisson’s ratio and Young’s modulus of steel, and k_f the foundation modulus due to ice, which is assumed to behave as a Winkler foundation. The pressure distribution along the line load for one individual frame is (again the x -coordinate is defined in an obvious way, i.e., in the direction normal to the frames and starting from a frame)

$$q(x) = \frac{1}{2} \cdot F_{tot} \cdot A \cdot e^{-A \cdot x} \cdot (\cos Ax + \sin Ax), \quad (12)$$

where F_{tot} is the total ice force acting on one frame – this can be defined as the rule requirement. For a long load patch, these contributions from each frame can be summed to give the final pressure distribution. The response of the plating under the total load distribution has been calculated (Riska & Windeler 1997, Uto 2000). The plate response was shown to depend on the rigidity factor R

$$R = A \cdot s. \quad (13)$$

The pressure model given by eq. (12) has been investigated in two laboratory test series in which the ice has been crushed against a framed structure and the forces and plate response has been measured (Lindholm et al. 1990, Tuhkuri 1993). The second set of tests provided the result that the foundation modulus k_f is about 2 GN/m^3 ; see Fig. 13. In the first test series, pressure distribution was measured directly; see Fig. 14. The latter results suggest that the rigidity factor is slightly above 2 GN/m^3 .

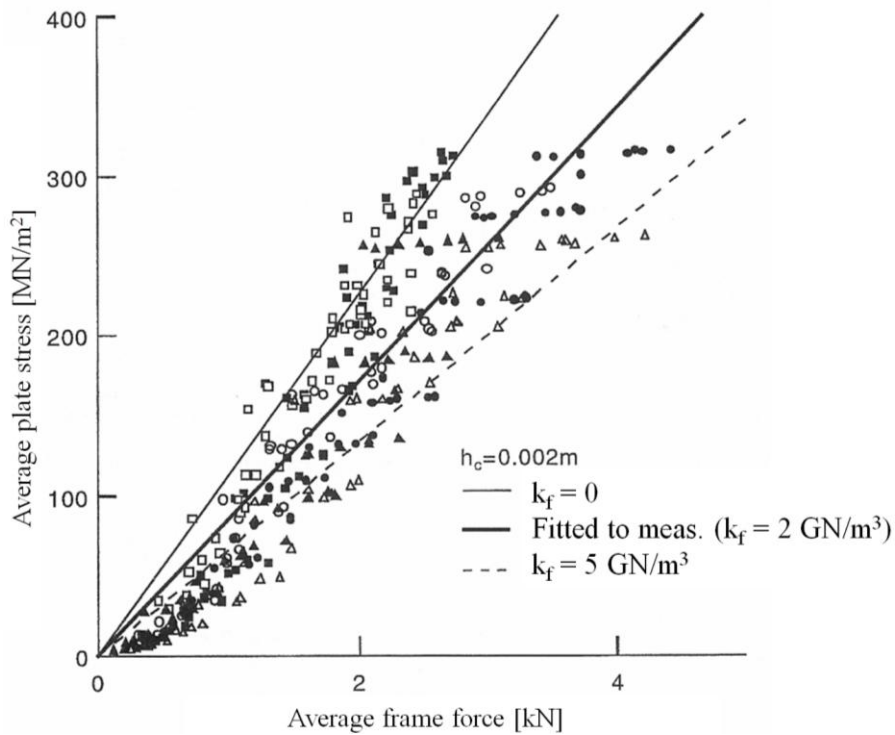


Fig. 13. Comparison of the measured and calculated stress response of a plate using different foundation moduli k_f (adopted from Uto, 2000, Fig. 16). In the calculation, the load height was small at 2 mm.

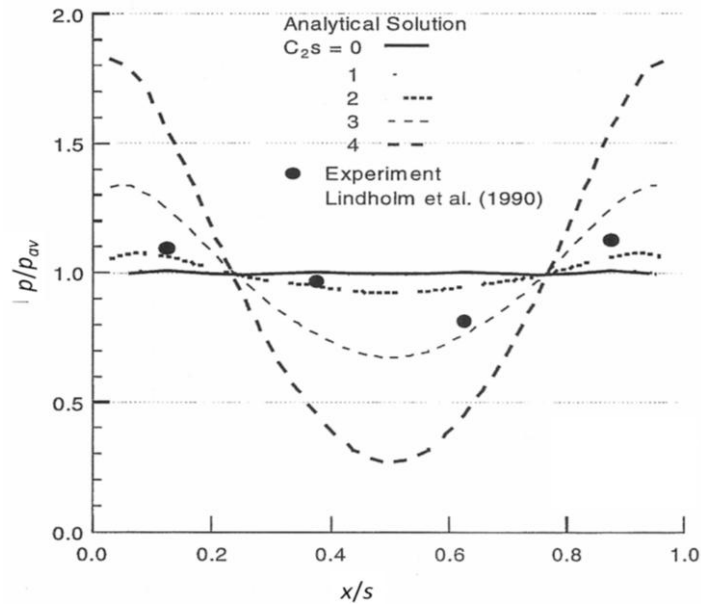


Fig. 14. Influence of the rigidity factor R (which, in this study, from which the figure was taken, was denoted as C_2) on the pressure distribution compared with measured pressures (Uto, 2000, Fig. 17). x is the coordinate normal to frames and starting on a frame.

The application of the above results is straightforward using eq. (12). Uto (2000) calculated the influence of the rigidity factor on the maximum plate stress and compared this with stresses caused by uniform pressure. From these calculations, the reduction factor for the equivalent plate pressure p_{PL} was obtained as given in Fig. 15, which also shows the present reduction factor in the rules.

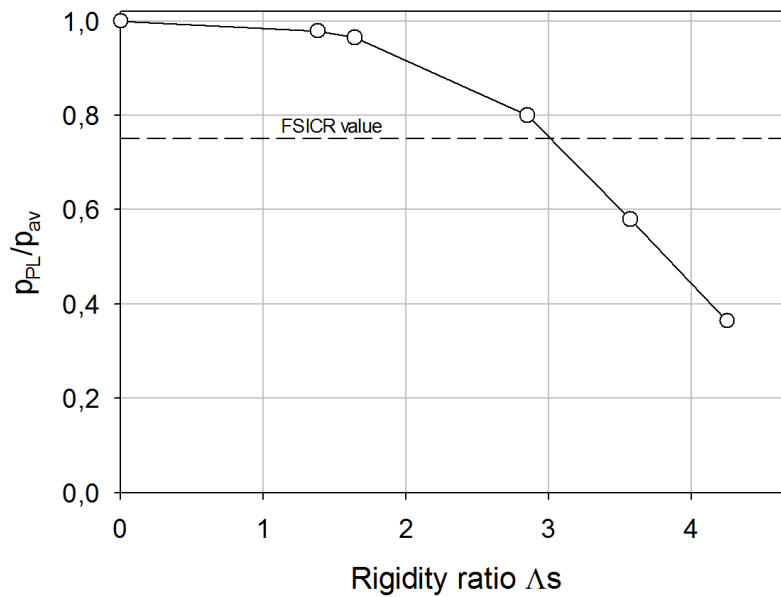


Fig. 15. Ratio between the effective plate pressure and the uniform pressure versus the rigidity factor Λ (Uto, Fig. 18b.)

The above results could be used in defining the reduction factor in a detailed fashion for the plating pressure in transverse framing systems. It was decided instead to use a constant in the FSICR that fits the measurements. The question of whether the pressure distribution is influenced in a similar way for longitudinally stiffened plating is open, but in the present FSICR the stiffness factor has been omitted from the longitudinally framed plating design.

4.5 Statistics of Ice Loads

The local ice loading process on the ship shell consists of separate peaks; see Fig. 16. Each of the peaks represents an impact with an ice edge at a separate cusp. This ice edge shape is formed by the breaking pattern by repeated breaking of these cusps. When the ship hits an ice cusp, the ice edge is first crushed and the contact force then increases with the contact area. The maximum force reached is determined by the bending strength of the ice cover. At any fixed location on the hull, the loading process, consisting of separate peaks, seems quite stochastic; this process has been described numerically by Su et al. (2010). The stochastic ice loading process must be described by statistical distributions – and it is natural to use the load distribution that is the distribution of the load peaks. Often, however, the maximum load values are described by the maximum value observed within some selected time period. Most of the Baltic ship ice load measurements that have been carried out for this period are either 12 h or 24 h.

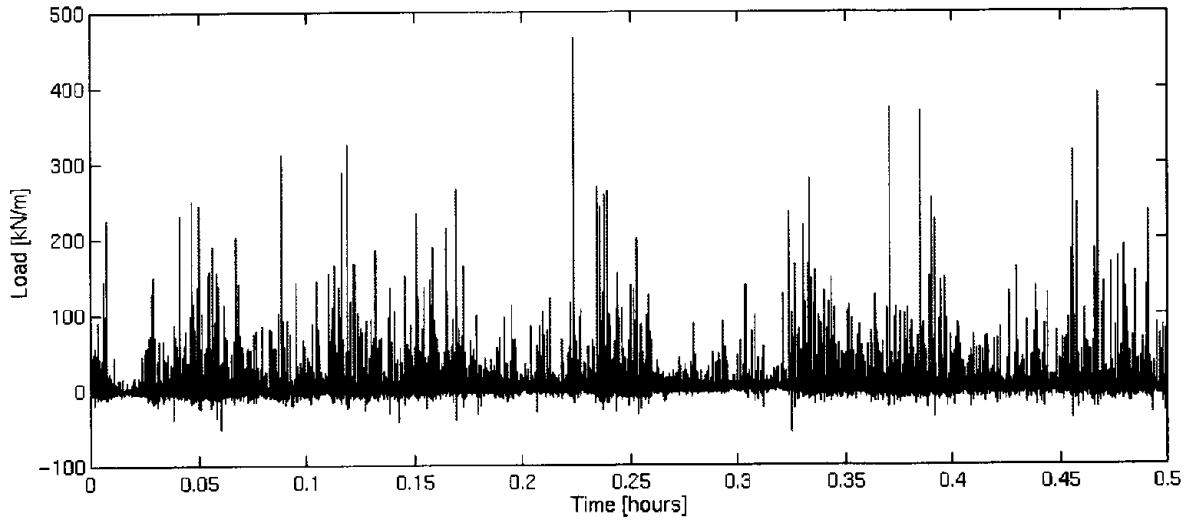


Fig. 16. A measured time series of the ice load on one single frame of the MT Uikku (Lensu 2002)

Before describing the probabilistic ice loads, the ice load distributions commonly used to describe the statistics of ice loads are explained briefly. If the probability distribution function (pdf) of the ice load peaks is denoted as $f_P(q)$, the corresponding cumulative distribution as $F_P(q)$, and the observed frequency of the peaks as ν_P , then the cumulative distribution of the maximum peak in the time period T is

$$F_T(q) = [F_P(q)]^{\nu_P T}, \quad (14)$$

assuming the peaks to be statistically independent. In principle, this expression can be extrapolated to any time period T , including the ship's lifetime. This kind of extrapolation is somewhat extreme, however, and at least the basic data in determining the $F_P(q)$ and ν_P should reflect the different ice conditions encountered during the ship's lifetime.

As mentioned above, often only the maxima from some measurement time period T_0 are available. These maxima can be used to determine the cumulative distribution $F_{T_0}(q)$ for the maximum for time period T_0 , which can then be extrapolated to the ship's lifetime T_L as

$$F_{T_L}(q) = [F_{T_0}(q)]^{T_L/T_0} = [F_P(q)]^{\nu_P T_L}. \quad (15)$$

The extrapolated distributions (from $F_P(q)$ to $F_T(q)$ or from $F_{T_0}(q)$ to $F_{T_L}(q)$) can be estimated using so-called asymptotic Gumbel distributions. These distributions capture the tails of distributions better than the original 'parent' distribution. The tails of probability distributions are important to design. Depending on the nature of the 'parent' distribution $f_P(q)$, three different Gumbel distributions, type I, II, and III, have been derived. Here, only the simplest, Gumbel I, distribution is used. The cumulative function of this distribution is

$$G(q) = e^{-e^{-c(q-u)}}, \quad (16)$$

where c and u are the parameters of this distribution. If the mean (q_{av}) and the standard deviation (σ_q) of the measured set $\{q_i\}$, $i=1, \dots, N$ are known, then the Gumbel I distribution parameters can be estimated using the moment method as

$$c = \frac{\pi}{\sqrt{6} \cdot \sigma_q} \quad (17)$$

$$u = q_{av} - \frac{\gamma}{c}$$

where γ is the Euler constant (value 0.5772...).

The asymptotic distribution can be used to derive a useful quantity that will subsequently be used, i.e., the return period T . This is the time period in which the maximum value for the peaks will exceed the most probable value of the distribution $g(q)$, where $g(q) = \frac{dG(q)}{dq}$. The return period corresponding to load q_T is defined as

$$T = \frac{1}{\nu_P} \frac{1}{1 - G_P(q_T)} \quad (18)$$

where the subscript T has been used to note that this is the most probable load value corresponding to the return period T . This expression will be used in the present investigation: when the $G(q)$ is the Gumbel I distribution of the maxima, each from a time period of length T_0 , the most probable load for the time period T is

$$q_T = u - \frac{1}{c} \ln\left(-\ln\left(1 - \frac{1}{T/T_0}\right)\right). \quad (19)$$

Instead of extrapolating the distribution of measured maxima, the basic, i.e., parent distribution, could be the peak distribution (subscript $T_0 \rightarrow P$).

The analysis of the design ice loading requires knowledge about the statistical properties of ice loads. The theoretical research into this matter is just commencing, so only knowledge that exists comes from measurements. The initial theoretical analysis (see, e.g., Su et al. 2010) suggests that the origin of the statistics of the local ice loading can be divided into two sources: external and internal. The external source is the variability of encountered ice conditions. The internal source is created by the variability of the breaking pattern of ice; this breaking pattern causes variations in the ice load even if the ice strength and thickness parameters would be constant. Here, however, only measured data are considered and the considerations are made somewhat more concrete by considering the measured data from MT **Kemira**.

MT **Kemira** is a chemical carrier that operates between the ports Kokkola and Uusikaupunki in Finland and central European ports. She visits Finland often, with a rotation of about one week. Her ice class is IA Super with a length of $L_{pp} = 105.0$ m, beam $B = 17.5$ m, power 3400 kW, and the deadweight is 5800 dwt. This ship was selected for measurements as she navigates regularly in the iciest conditions in the Baltic – thus her operational spectrum can be assumed to represent a typical Baltic merchant ship of her size and shape, naturally. **Kemira**'s ice load data are described by Kujala (1989), Gylden and Riska (1989), and Muhonen (1991, 1992).

MT **Kemira** was instrumented to measure the ice load on one frame (labeled FFR in Fig. 17) as well as the plate and frame stresses (labeled PL and FN). The frame load measurement was carried out using shear strain gauges attached at the neutral axis of the frame: the difference between the two shear stresses on the same frame is proportional to the load on the frame between these gauges.

The ship and measurement locations are shown in Fig. 17. The data used from MT **Kemira** include the frame loads denoted by F [kN]; these were measured at the bow, midship, and stern areas of the ship hull, at two or three draughts. The stern load measurement location is actually at the stern shoulder, i.e., at the boundary between the midship and stern hull area.

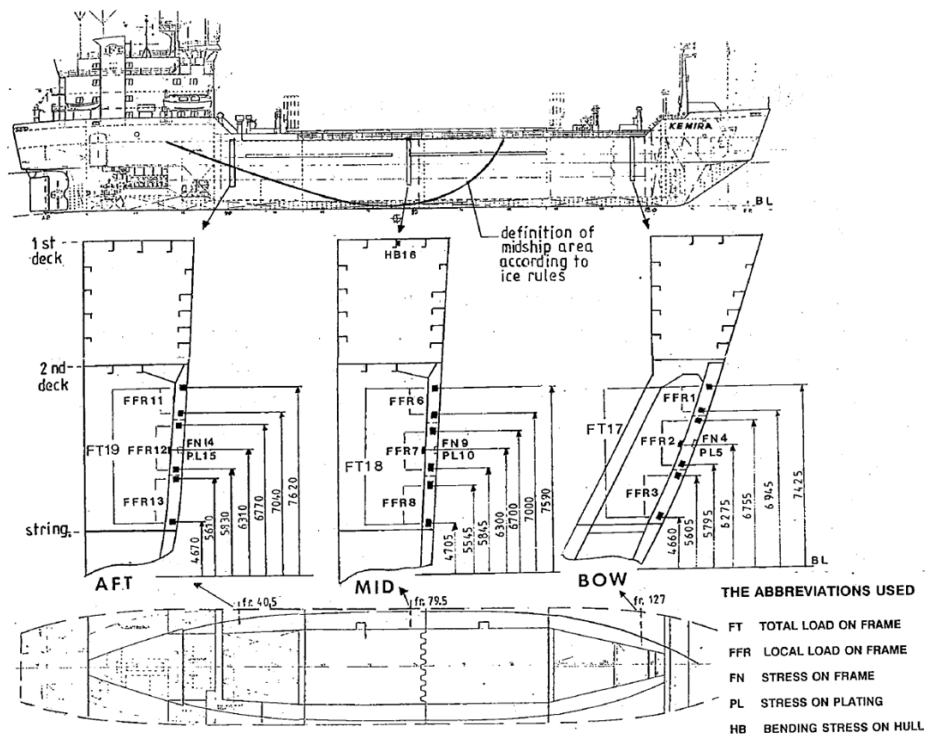


Fig. 17. Ice load measurement system installed onboard MT **Kemira** (Kujala 1989)

The measurement system does not record the time histories of the signals but, instead, calculates two histograms for each measurement channel and measurement period. One histogram consists of the digitized samples from each measurement channel with a sampling rate of 100 Hz. The other histogram includes the ice force peaks, with each peak calculated using the Rayleigh separation for the peaks (with 25% of the peak value as the separator). These histograms were stored after each 12 h period throughout the winter for the years 1985-1991.

The data used here are derived from the maxima of each 12 h peak distribution. Only the maxima from periods when the ship was sailing in ice are included. Before using the data, some processing has to be done. The first assumption was to omit the smallest peaks, as these most probably contain some electronic noise as well as very small ice-induced responses. Specifically, peaks smaller than 20 kN are ignored. The other assumption was to collate the data so that from each 12 h period, the maximum frame load of the measured peaks at the same frame was taken to the data. Thus, the data consist of $\text{MAX}[\text{FFR1}, \text{FFR2}]$, $\text{MAX}[\text{FFR6}, \text{FFR7}]$, and $\text{MAX}[\text{FFR11}, \text{FFR12}]$, where FFR stands for frame load in the gauge denotation used in the measurements; see Fig. 17.

The data used are in the form of histograms for bow, midship, and stern frame loads. The measured load is converted into a line load by dividing the measured force F by the frame spacing ($q = F/s$, $s = 35$ cm), thus the basic data are in the form of $\{q_i\}$, $i=1, \dots, N$ where each q_i is from some 12 h period during years 1985-91 and N is the total number of 12 h periods included in the data. In order to use the data in the subsequent analysis, the Gumbel I distribution is fitted to the data. The data and the fits are presented in Table 6. The data and the Gumbel fits are shown in Figs. 18a to 18c, which also give the design load values according to ice class IA Super in the FSICR. The plots

versus the return period were made by plotting q versus $T(q_i) = \frac{1}{v_0} \frac{N+1}{N+1-i}$ where $v_0 = 1/(0.5 \text{ day}) = 2/\text{day}$. The bow, midbody, and stern rule load values correspond to the return periods of 5 days, 7 days, and 5 days, respectively. These values seem low, and the design point is investigated in Chapter 6.

Table 6. Data about frame ice loads

Quantity	Bow	Midship	Stern
No. of points N	304	309	388
Mean [kN/m]	460.2	241.3	244.6
STD [kN/m]	334.6	178.4	203.8
Gumbel para. c [m/kN]	0.00383	0.00719	0.00629
Gumbel para. u [kN/m]	309.7	161.0	152.9

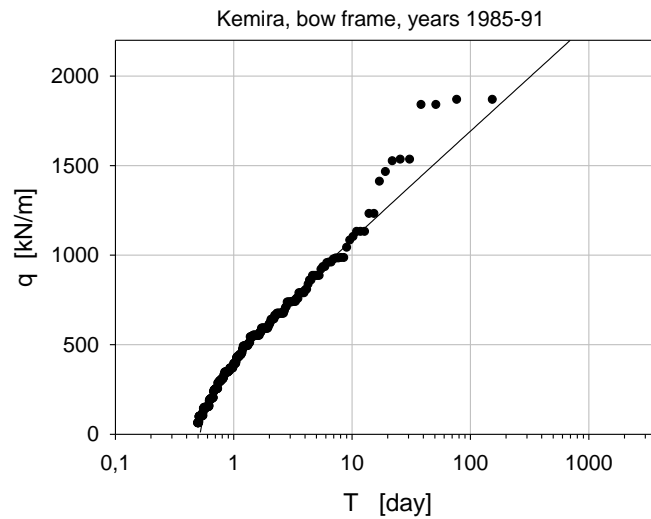


Fig. 18a. Measured and estimated (according to Gumbel I pdf) loads versus the return period for bow frame loads. The IA Super Rule value is 790 kN/m.

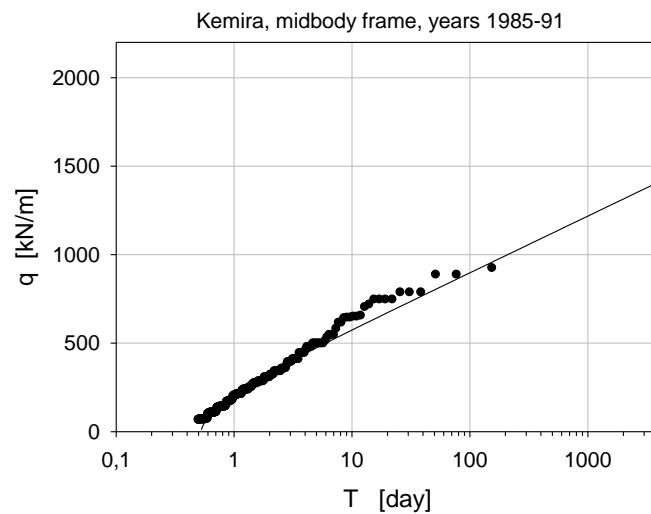


Fig. 18b. Measured and estimated (according to Gumbel I pdf) loads versus the return period for midship frame loads. The rule value is 510 kN/m.

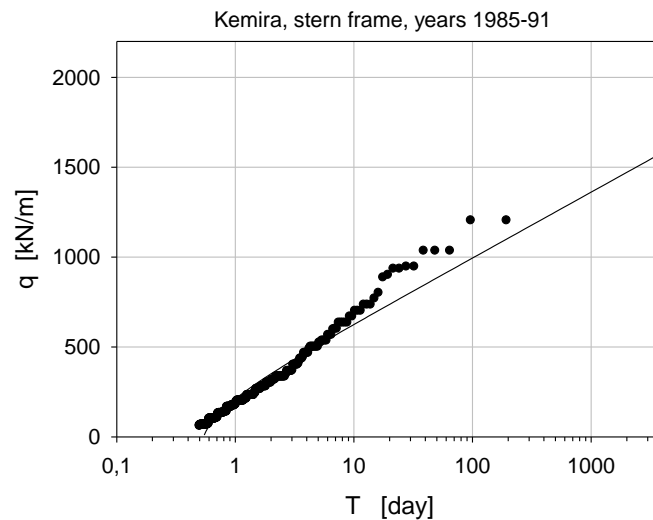


Fig. 18c. The measured and estimated (according to Gumbel I pdf) loads versus the return period for the stern frame. The rule value is 380 kN/m.

The advantage of using the Kemira data from these seven years is that they integrate different winters (three severe, two average, and two mild) as well as the ice thickness development during each winter. The disadvantages include the dependency on MT **Kemira's** size, hull shape, and navigation spectrum (MT **Kemira** mostly visited the ports in Uusikaupunki and Kokkola in Finland). The fact that during each 12 h period the ship did not navigate in ice the whole time – in fact, the ice navigation was less than 12 h for most of the 12 h periods (see Muhonen 1992, Appendix 3). This effect has been investigated by Hänninen (2002): the effect was noted to be quantitatively important but did not change the data qualitatively.

In order to have some insight into the data, the statistical distributions are investigated briefly. The basic distribution is the distribution of peaks, $f_P(q)$, from a time period of 12 h. The bow frame load data from 3/16/1991 (A.M.) are used for this demonstration, data from Muhonen (1992). On this day, the ship was operating through the Quark having left Kokkola at midnight. The maximum undeformed level ice thickness during this time and in this area was about 50 cm. These data and the Gumbel I distribution fitted to the peaks are shown in Fig. 19 (the Gumbel I parameters are $c = 0.0152$ m/kN and $u = 85.6$ kN/m). It is quite clear that the Gumbel distribution underestimates the number of large peaks.

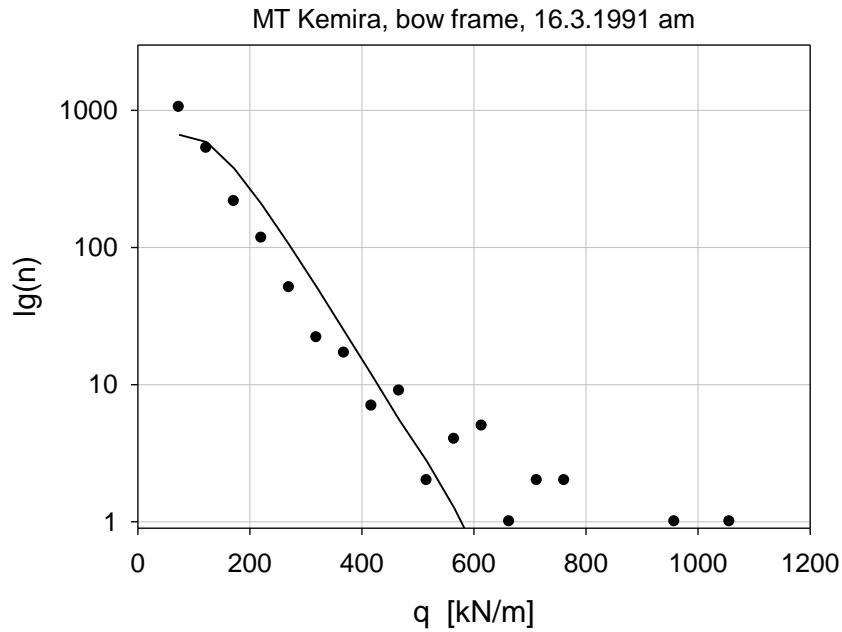


Fig. 19. Measured histogram of peaks on 3/16/1991 (A.M.) and the fitted Gumbel I distribution on semi-logarithmic coordinates. The number of peaks in each histogram bin of width 50 kN/m is n .

It is also of interest to compare the distribution fitted to the measured 12 h period maxima with the extrapolated distribution derived from the measured peak histogram from 16 March (A.M.). The comparison is shown in Fig. 20. The extrapolated Gumbel distribution of the peak distribution to the whole measurement period (ν_P is 313.8 1/h, i.e., $N = 3770$). The extrapolation gives the most probable maximum during the time $T = 12$ h

$$F_T(q) = [F_P(q)]^N = e^{-e^{-0.0152(q-625.3)}}, \text{ unit of } q \text{ kN/m.} \quad (20)$$

This distribution can be compared with the one derived from the whole data set: the pdfs calculated from $F_P(q)$ are compared with the pdf from the 12 h maxima in Fig. 20. The fit to the 12 h maxima gives a far wider distribution, which is clear, as all kinds of ice conditions are included in the data whereas the extrapolated peak distribution is quite sharp with a most probable value of about 630 kN/m. This difference is natural as the ice conditions on 16 March correspond to the most severe annual ice conditions.

This short analysis of the maxima from a single measurement campaign raised some questions concerning the extrapolation of loads and the connection of the estimated pdfs to ice conditions. It would be interesting to study the relationships between the peak distribution, distribution of maxima from certain time periods, and the method of extrapolation to lifetime values. This falls outside the focus of the present article, however, and warrants a study in itself.

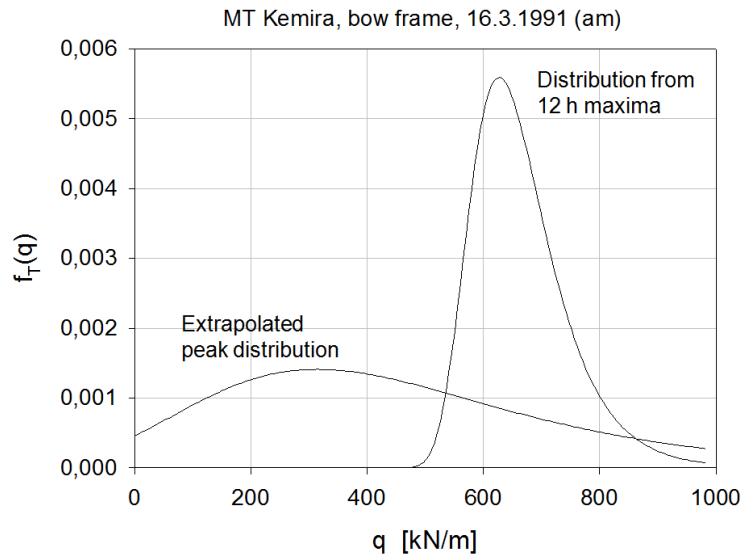


Fig. 20. Extrapolated peak distribution for a 12 h period (right pdf) compared with the distribution from the 12 h maxima from the years 1985-91 (left pdf)

To conclude the study of the statistics on ice loads, the ice load measurement results from measurements carried out with four different vessels in the Baltic are described; see Hänninen (2002). The results of a statistical curve fit using the Gumbel I extreme value distribution on the data from these four ships are shown in Fig. 21. The load q is presented versus the return period T of the load. As the statistical distribution used is Gumbel I, the most probable maximum load from period T is given in Eq. (19). The statistical parameters are given in Table 7 for the cases shown in Fig. 21. It is noteworthy that the values of the constant α , which are proportional to the standard deviation of the distributions, are very close to each other. The values from the northern Baltic (**Sisu** and **Kemira**) and values from the Gulf of Finland (**Arcturus** and **Kashira**) are also very close to each other, respectively. These observations would warrant closer investigation.

Table 7. Statistical quantities for the four different ice load measurements, $[T] = \text{day}$

Measurement	Gumbel I parameters		Load when $T = 1000$ days
	u [kN/m]	c [m/kN]	
IB Sisu	680	0.0043	2290 kN/m
MS Arcturus	500	0.0050	1880 kN/m
MT Kemira	780	0.0045	2310 kN/m
MT Kashira	310	0.0047	1780 kN/m

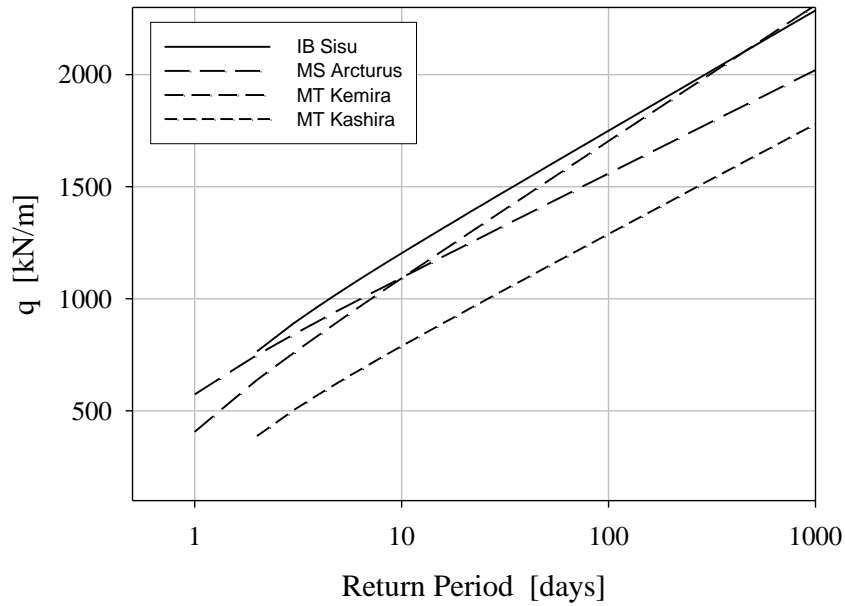


Fig. 21. The fitted Gumbel I distributions of the ice load on one vertical frame obtained from four measurement campaigns plotted versus the return period of the load

The loads given in Table 7 corresponding to a return period of 1000 days are quite high compared with the rule values. The time period of 1000 days represents a typical time spent in ice for a merchant vessel regularly visiting Finnish ports year-round during her lifetime. These values could be compared with the line load value given by the nominal ice pressure p_0 ; $q_0 = 1960$ kN/m (ice class IA Super). Another way of looking at the measured loads is to calculate the return period that corresponds to the design line load according to ice class IA Super. These are given in Table 8. The difference in the return period for ships navigating to the Bay of Bothnia and Gulf of Finland is clear. The yield limit is exceeded for ice class IA Super sailing to the ports in southern Finland roughly once per winter.

Table 8. Return period to give the same load as the design load in ice class IA Super

Measurement	Frame design load in ice class IA Super [kN/m]	Return period of the design ice load [day]
IB Sisu	1160	8.9
MS Arcturus	1160	14.6
MT Kemira	790	3.5
MT Kashira	950	21.5

The balance between the selected design return period and the limit response caused by the load corresponding to the design period must be found in some way. This balance of the limit response and frequency of reaching this limit response is analyzed in Chapter 6.

5. STRUCTURAL RESPONSE

The response in terms of the maximum stress of plating and frames is investigated briefly in order to analyze the design point using different limit states in Chapter 6. Several studies have been carried out investigating the plastic and ultimate response of ship hull structures under ice loads – one of the first ones is Johansson (1967). The other studies include studies in the project SAFEICE (Kujala, ed. 2007), and damage studies Varsta et al. (1978), Ranki (1986), Hayward (2001), Daley (2002a,b), Valkonen (2006), and Kaldasaun (2010). The development of formulations for the elastic and plastic response of plating and frames would be a main topic in itself; here, only some formulations are selected for use in investigating the design point.

5.1 Plate Response

In order to calculate the elastic response of plating, the formula developed for the Finnish-Swedish ice class rules (Trafi 2010) can be used. The relationship between ice loading q and load height h , plate stress σ and scantlings (t plate thickness and s frame spacing) for transversely frame structure is

$$p_{PL} = \frac{9}{4} \cdot \left(\frac{t}{s}\right)^2 \frac{\sigma}{1.3 - \frac{4.2}{(h/s + 1.8)^2}}. \quad (21)$$

The equivalent pressure on plating is denoted as p_{PL} , which is the uniform pressure at load height h that gives the maximum stress σ . The factor in the denominator takes into account the load height effect at constant line load value.

The plastic response formulation of plating is taken from Hayward (2001). Hayward (2001) conducted a large set of FE-calculations of plastic response of plating and the results are deemed most reliable and robust to be used here. The line load to cause a fully plastic response with no permanent deflection ($w_P = 0$) is thus described by (L is the frame span):

$$p_P = \frac{16 \cdot t^2 \cdot \sigma_y}{s^2 \left(\sqrt{3 + \left(\frac{s}{L}\right)^2} - \frac{s}{L} \right)^2} \cdot \frac{1}{0.6701 \cdot \left(\frac{h}{s} \cdot \left(\frac{s}{t}\right)^{0.2}\right) - 0.1330 \cdot \left(\frac{h}{s} \cdot \left(\frac{s}{t}\right)^{0.2}\right)^2}, \quad (22)$$

where σ_y is the yield stress and the constant 0.75 has been accounted for in the multiplicative factor on the right-hand side. The ice pressure to cause the ultimate response is given as

$$p_U = p_P \cdot \left[1 + \frac{w_P^2}{3 \cdot t^2} \left(\frac{\zeta_0 + (3 - 2 \cdot \zeta_0)^2}{3 - \zeta_0} \right) \right] \text{ when } w_P/t \leq 1 \quad (23)$$

$$p_U = 2 \cdot p_P \cdot \frac{w_P}{t} \left[1 + \frac{\zeta_0 \cdot (2 - \zeta_0)}{3 - \zeta_0} \cdot \left(\frac{t^2}{3 \cdot w_P^2} - 1 \right) \right] \text{ when } w_P/t > 1, \quad (24)$$

where the permanent deformation is w_P and

$$\zeta_0 = \frac{s}{L} \cdot \left(\sqrt{3 + \frac{s^2}{L^2}} - \frac{s}{L} \right).$$

5.2 Framing Response

The equations corresponding to the plating response, especially for the plastic frame response, are more complicated than the corresponding ones for plating. The different boundary conditions of continuous beams and end brackets cause variation as well as different deformation mechanisms. If only pure bending deformation is taken into account, the formulation is often too simple, as at least the shear deformation should also be taken into account. There is no clear formulation for the inclusion of shear deformation, and as there is quite great uncertainty in describing the ice loads, the frame response in this study is obtained by only describing the simple bending response.

When a frame is considered as a clamped beam (span L) and loaded at the midspan by a patch load of height h with the ice load $q \cdot s$, then the bending moment at the supports is

$$M = \frac{(3 \cdot L^2 - h^2) \cdot C_l \cdot p \cdot h \cdot s}{24 \cdot L}, \quad (25)$$

where the coefficient C_l takes into account the support of the adjacent frames. The value of this coefficient depends on the load length as well as the plate thickness and frame spacing. The value of the coefficient must be 1.0 if the load length is large, i.e., covers more than, for example, the frame spacings. The value for the coefficient C_l is derived by comparing measured loads and frame response in the Kemira data. In plastic calculations (Varsta et al. 1978), in which only a single frame of a multi-frame structure was loaded, the support effect has been observed to give a value of $C_l = 0.55$, i.e., almost half of the load is supported by adjacent frames. Here, a value $C_l = 0.65$ is used – this is obtained by comparing the measured frame loads and frame stresses; see Riska (2011).

The displacement at the middle of the beam corresponding to (25) is

$$\delta = \left(2 \cdot L^3 - 2 \cdot L \cdot h^2 + h^3 \right) \cdot \frac{C_l \cdot p \cdot h \cdot s}{384 \cdot E \cdot I}, \quad (26)$$

where E is the Young's modulus and I the section moment of inertia.

When the maximum stress reaches yield, an expression for the elastic limit pressure p_Y (and line load q_Y) is obtained as

$$C_l \cdot q_Y = C_l \cdot p_Y \cdot h = \frac{24 \cdot L}{(3 \cdot L^2 - h^2) \cdot s} \cdot \sigma_y \cdot Z_e. \quad (27)$$

where L is the frame span and Z_e (elastic) section modulus. This simple equation can be compared with the equation in the FSICR, which states that the load causing yield is (in FSICR $C_l = 1$):

$$C_l \cdot q_Y = \frac{7 \cdot m_0}{7 - 5 \cdot h/L} \frac{Z_e \cdot \sigma_y}{s \cdot L}, \quad (28)$$

where m_0 is a boundary condition factor between 5 and 7. These equations give very similar results.

As the loading increases from the load that causes the first yield, the stress distribution at the supports includes increasing amount of plastic (yield) stress, and two hinges are formed at the supports when the stress distribution is fully plastic. At this instant the pressure (and line load) is

$$C_l \cdot q_P = C_l \cdot p_P \cdot h = \frac{24 \cdot L}{(3 \cdot L^2 - h^2) \cdot s} \cdot \sigma_y \cdot Z_P, \quad (29)$$

where Z_P is the plastic section modulus. The deformation corresponding to the pressure in Eq. (29) can be obtained by inserting this pressure into Eq. (26).

When the stress distribution at the supports is fully plastic, the supports start to act as hinges. When the loading increases further, the beam behaves as a simply supported beam. Eventually, the stress distribution at the mid-span reaches a fully plastic state. At this instant, three hinges are formed and the frame is assumed to collapse if the material is assumed to behave as elastic – ideally plastic. The additional pressure (additional to p_P) causing the three hinges is obtained by setting the sum of the moment of a clamped beam at the mid-span due to the pressure in Eq. (29) and the moment caused by the additional pressure (p_{add}) of a simply supported beam equal to $M_Y = \sigma_y \cdot Z_P$ ($M_Y = M_C(p_P) + M_{SS}(p_{add})$ where the subscript C refers to clamped and SS to simply supported). This way, the ultimate pressure (and line load) for a frame is obtained as

$$C_l \cdot q_U = C_l \cdot p_U \cdot h = \frac{16}{s \cdot (2 \cdot L - h)} \cdot \sigma_y \cdot Z_P \quad (30)$$

and the corresponding displacement at the mid-span as

$$\delta_U = \frac{12 \cdot L^5 + 18 \cdot L^4 \cdot h - 28 \cdot L^3 \cdot h^2 + 8 \cdot L \cdot h^4 - 2 \cdot h^5}{48 \cdot (2 \cdot L - h) \cdot (3 \cdot L^2 - h^2)} \cdot \frac{\sigma_y \cdot Z_P}{E \cdot I}. \quad (31)$$

A reference for this formulation is Hayward (2007). The frame response formulation is simple, as it does not consider the shear deformation or the material post-yield behavior. In order to check the validity of the frame plastic formulation, the results in Eqs. (27-30) are compared with results from FE calculations conducted by Det Norske Veritas (Holtmark & Strömme 2004). The results of the comparison are shown in Fig. 22 (as only one frame was investigated, $C_l = 1$).

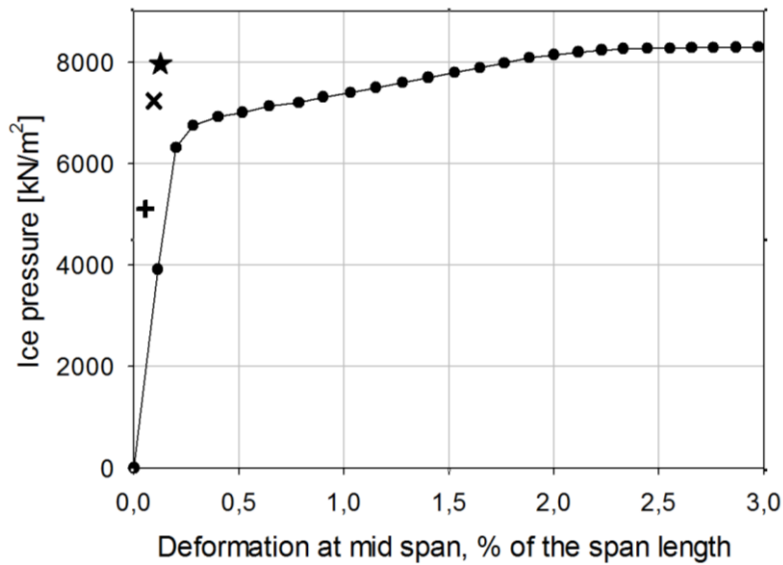


Fig. 22. Comparison of the results of the simple derivation with FE calculations (Holtmark & Strömme 2004). The plus, cross, and asterisk represent the elastic, plastic, and ultimate limits, respectively, derived in this article. The frame span is 1.8 m. Other quantities are $s = 40$ cm, $h = 40$ cm, $Z_e = 716$ cm³, $Z_p = 1005$ cm³, and $I = 17310$ cm⁴.

The comparison shows that the displacements given by the simple formulations are smaller than those obtained by FEM. The pressure values are quite reasonable however. Further validation is given by the collapse equation for frames developed by Ranki (1986); this gives the ultimate pressure of 10.3 MPa for the first case ($L = 1.8$ m) and 8.3 MPa for the second case ($L = 2.4$ m). These are about 5% higher than those given by (30). Thus, the present simple formulae can be and are used in this study.

6. DESIGN POINT IN THE ICE RULES

6.1 Description of the Design Point

The aim of the structural response formulations in Chapter 5 is to derive a relationship between the limit response, the scantlings, and the load. Here, only a transversely framed hull structure is investigated. The limit response that is investigated includes both elastic and plastic limit states. More precisely, the limit states that are investigated include the cases shown in Table 9.

Table 9. Definition of the limit states for plating and frames

Limit state (label)	Plating	Frames
Elastic (Y)	Stress reaching the yield stress σ_y somewhere in the plate	Stress reaching the yield stress σ_y somewhere in the frame
Plastic (P)	Stress distribution reaching full plasticity somewhere in the plate; Permanent deformation still zero	2-hinge formation at the frame supports
Ultimate (U)	Permanent deformation (w_p) reaching a specified value	3-hinge formation at the frame supports and the mid-span

The reason the permanent deformation is specified for plating but not for frames is that no easy formulations are available for frame deformation, and the simple formulation gives deformation that

is too small. Some formulations for frame deformation exist, like the one given in NORSOK N-004 (Appendix A, section 3, eq. A.3.28), but it was decided to use only loading for simple 2- and 3-hinge formulations for this scoping study. These also ignore shear deformations. The plastic reserve due to membrane stresses is large for plating, and simple formulations for the permanent deformation of patch-loaded plates exist (see, for example, Hayward, 2007)

The concept of the design point includes a definition of the limit state and the frequency with which this limit state is reached, assuming a certain operational spectrum for the ship. The limit state function $L(Q, q)$ includes the load q (which is determined by the operational spectrum) and the strength of the structure Q (determined by scantlings, material properties, and geometry) – the latter is often expressed as the load causing a response up to the selected structural limit. The structural limit in the following analysis will either be stress reaching yield stress somewhere in the structure; full plasticity, i.e., at some point in the structure the stress distribution is fully plastic; or some specified permanent deformation – or for frames, collapse. If the limit is denoted as w (being Y, P, or U, respectively) and the structural details (scantlings etc.) as d – this can be a vector, i.e., contain more than one parameter – then the limit state (which is commonly called ‘strength’ of the structure) can formally be presented as

$$q = f(w, d). \quad (32)$$

At the same time, equations like Eq. (17) give the most probable load in a given time, i.e., the return period T as

$$q = g(T). \quad (33)$$

If the Gumbel I distribution is used for the load, the load versus the return period is obtained by starting from Eq. (17). The strength and statistics of the ice loading can be combined to give the design equation (solving for d from $g(T) = f(w, d)$):

$$d = h(w, T). \quad (34)$$

This process of determining the scantlings is sketched in Fig. 23 in which equation (32) is on the left-hand side and equation (33) on the right-hand side. The aim now is to investigate the influence of w and T on d . For example, it is of interest to check what combinations of w and T give the same scantlings.

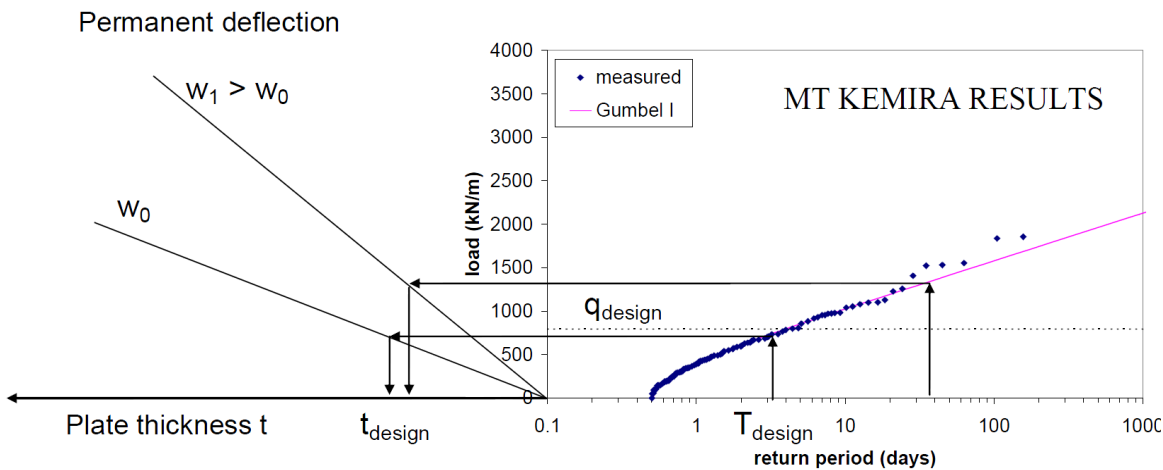


Fig. 23. A sketch of the design point definition (Riska 2007)

In principle, Eq. (34) can be obtained by combining the load formulation given in Chapter 4 and the limit state formulations given in Chapter 5. The resulting formal equations would not, in themselves, give much insight; thus the whole analysis is made using MT **Kemira** as an example. This way, the values of most of the scantlings like the frame spacing, frame span, frame boundary conditions, and the yield strength of the steel can be fixed. Thus, the frame spacing used in the subsequent analysis is $s = 35$ cm, frame span $L = 3.5$ m, and yield strength $\sigma_y = 235$ MPa.

Three different hull areas are investigated: bow, midship, and stern, using the measured loading as representative for these areas. This is not strictly correct, as the bow, as well as the stern area, contains a range of hull angles. The stern measurement position is where the frame angle is almost vertical – thus these loads can be considered conservative for what influences the hull shape. The bow load measurement position is where the waterline angle is $\alpha = 19^\circ$ and the frame angle is $\beta = 24^\circ$. This position is at about the centre of the bow area length and thus the measured loads can be considered characteristic of the whole **Kemira** bow, on average.

The ice class of MT **Kemira** is IA Super. The calculated scantlings are compared with the minimum values required by the Finnish-Swedish Ice Class Rules (Trafi 2010) and the ice class PC6 of the International Association of Classification Societies Polar Class Rules (IACS 2007). These two classes are generally considered as approximately equivalent – this equivalency is one of the motives of this study, as the limit state in the design point in the Finnish-Swedish Ice Class Rules is the yield (Y) limit state and in the IACS rules it is a plastic limit state (either fully plastic or ultimate, it is not clear which one is used). The required scantlings of MT **Kemira** for these two classes are given in Table 10. It should be noted that the required section modulus for the ice class PC6 is a plastic section modulus while for ice class IA Super, it is elastic. The plate thickness given is the net thickness.

Table 10. The required scantlings for MT **Kemira** (both the elastic and plastic section modulus are given for MT **Kemira**, denoted as Z_e / Z_p).

Hull area	Scantling	IA Super (Z_e)	PC6 (Z_p)	Kemira, as built
Bow	Z [cm ³]	713	3100	773 / 1010
	t [mm]	17.4	18.0	21
Midship	Z [cm ³]	412	1230	390 / 553
	t [mm]	13.9	11.8	16
Stern	Z [cm ³]	309	1094	384 / 490
	t [mm]	12.1	11.1	16

6.2 Design Point Calculations

When the load statistics and strength equation have been derived, the required scantlings can be determined versus the return period using the limit state as a parameter. This plot for plate net thickness for the bow is shown in Fig. 24 – using MT **Kemira** as an example. This plot also shows the required net plate thickness according to ice class IA Super and PC6. Similar plots can be made for the midbody and stern hull regions.

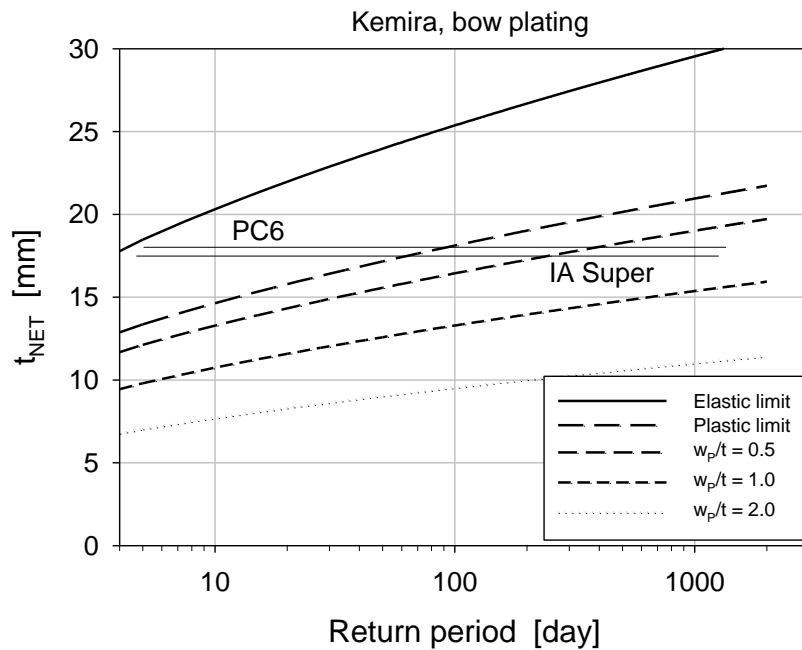


Fig. 24. Plate thickness corresponding to different limit states plotted versus the return period, bow area. w_p , in the legend is the permanent deflection of the plate.

A similar plot of the elastic section modulus versus the return period, using the limit state as a parameter, is shown for the bow hull region in Fig. 25. Again, similar plots can be made for the other hull regions. These plots are made using the geometry of the shell structure of MT **Kemira**. The section modulus shown is the elastic section modulus – the plastic section modulus obtained from the plastic analysis is converted to the elastic one using the ratio of plastic to elastic section modulus of MT **Kemira** frames ($Z_p/Z_e = 1.31$ for bow frames, and 1.43 and 1.28 for the midship and stern frames, respectively).

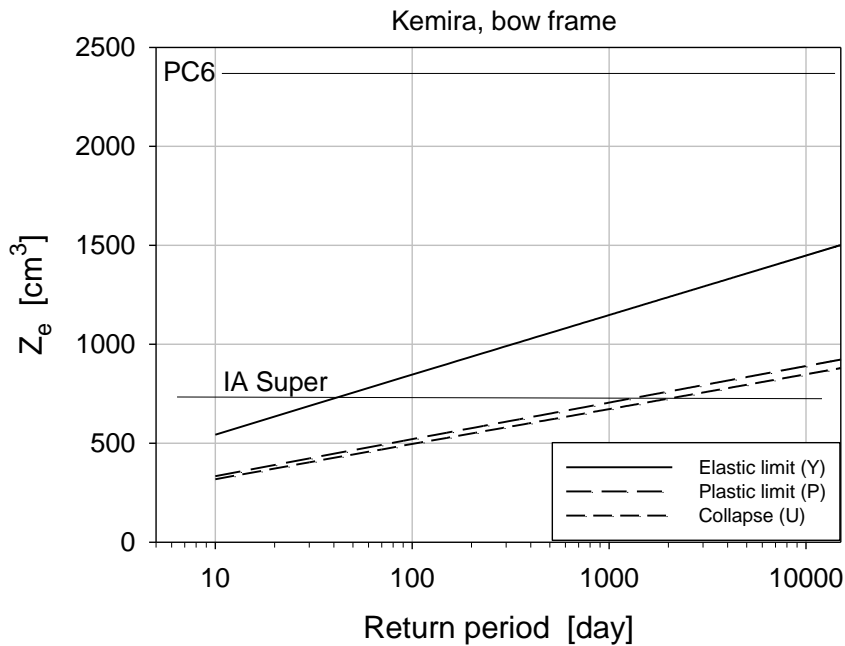


Fig. 25. Frame elastic section modulus corresponding to different limit states plotted versus the return period, bow area

6.3 Design Point

The calculations shown in Section 6.2 can be used to compare the scantlings required by the ice classes IA Super and PC6. This is done by determining the required plate thickness or frame section modulus and comparing these with those thicknesses or frame section moduli corresponding to the different limit states once in the ship's lifetime (1250 days in ice per lifetime). These values are presented in Table 11. It is immediately clear that the built scantlings correspond closely to the plastic limit state, whereas the scantlings given by the IA Super requirements correspond to some permanent deformation of the plating and to about 2-hinge formation for framing. The plate thickness for the midbody and stern hull regions required by the ice class PC6 seem to be somewhat low as dents as deep as the plate thickness are allowed.

Table 11. Calculated scantlings corresponding to different limit states once per lifetime compared with (net) scantlings required by the ice class. The plastic section modulus is converted into the elastic one.

Scantling	Hull area	Required by ice class		As built	Corresponding to a limit state with $T = T_L$	
		IA Super	PC6		Yield (Y)	Plastic (P)
t [mm]	Bow	17.4	18.0	21	29.9	21.2
	Midbody	13.9	11.8	16	22.9	16.4
	Stern	12.1	11.1	16	23.0	16.4
Z_e [cm ³]	Bow	713	2370	773	1170	715
	Midbody	412	860	390	622	347
	Stern	309	860	384	694	437

Finally, the calculations can be used to determine which scantlings are required if the return period is one year or the ship's lifetime and the corresponding limit states yield (Y) or fully plastic response (P). The comparison is shown in Table 12. It is apparent that the built scantlings correspond closely to the plastic limit state once per lifetime, whereas the frames are somewhat stronger. These two cases are also very close to each other.

Table 12. The required scantlings for two design points (Y, once per year; P, once per lifetime)

Limit state	Return period	Structural member	Hull area		
			Bow	Midbody	Stern
Yield (Y)	1 year	Plate t [mm]	23.5	17.5	18
Plastic (P)	Lifetime		21.5	16	16.5
Yield (Y)	1 year	Frame Z_e [cm ³]	570	400	450
Plastic (P)	Lifetime		560	360	460

7. FUTURE CONSIDERATIONS

All ice class rules, including the Finnish-Swedish Ice Class Rules, need updating when a new insight into the ice loading, structural response, or design point is obtained. A sound development environment would be one in which the rules were critically appraised quite often by including new knowledge of the loading and investigation, if all possible structural responses had been taken into account. The feedback from the built ships is also important and a systematic way to collect the

feedback in the form of ice damage should exist. If it relied only on the feedback from the practice (ice damage) and this feedback urged changes in the loading, structural response formulations, or design point, then the changes would be somewhat arbitrary – at worst this could lead to ‘design by disaster.’ Here, only two possible items to be taken into account in the future development of the FSICR are mentioned: that of the hull shape in determining the ice loads and the validation of the design point.

7.1 Hull Shape Effect on Ice Loads

A recent research project, SAFEICE, produced two slightly different results from the influence of hull angles. The theoretical calculations given in Valanto (2005) suggested that the influence of hull lines is, at most, quite small, as there are two competing physical processes that influence the hull angle dependency. The waterline angle α influences the indentation speed into ice and the normal frame angle β_n influences the amount of the total force that is required to bend the ice. The hull ice load measurements on a model scale (Izumiyama 2005) suggested that the ice load is inversely proportional to β_n , i.e.:

$$F \propto \frac{1}{\beta_n}. \quad (35)$$

The normal frame angle β_n can be obtained from α (waterline angle) and φ (buttock line angle). The relationship giving the normal frame angle is

$$\tan \beta_n = \frac{\sin \alpha}{\tan \varphi}. \quad (36)$$

In order to investigate the influence of hull lines on the contact force, some formulations to account for the hull angles are investigated here. Four different ships, from which there are full-scale data (IB **Sisu**, MV **Arcturus**, MT **Kemira**, and MT **Kashira**), are used as a comparison. The hull angles of these vessels, at the location where the loads were measured, are given in Table 13. The angles used are shown in Fig. 26.

Table 13. Hull angles of ships used in the comparison [degrees]

Ship	α	φ	β	β_n
IB Sisu	23	20	49	46.6
MV Arcturus	16.5	29	28.2	27.2
MT Kemira	19	40	22.4	21.3
MT Kashira	20	44	20.7	19.5

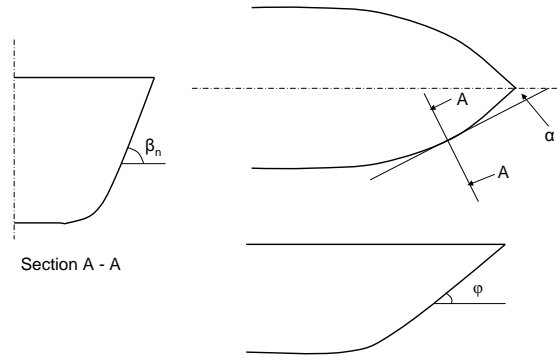


Fig. 26. Definition of the hull angles

The first method to account for the hull angles in determining the ice loads that are considered here is suggested in Kujala (1994). It is based on the observation that the frame load F is proportional to the normal frame angle in the measurements with MT **Kemira**, as follows (angle in degrees):

$$F \propto \beta_n^{-1.46}, \text{ if } \beta_n > 15^\circ. \quad (37)$$

This dependency is valid down to normal frame angle values of about 15° , as when the frame angle becomes smaller than this limit, ice is not broken by bending but rather by crushing (this bending/crushing limit also depends on the coefficient of friction between the ice and the hull).

This formulation for shape effect is just one of many. One strong assumption using the above formulation is that the force is related to hull angles in a similar fashion in all ship-ice interaction scenarios included in the measurements, i.e., when ice is failing in bending, when the load is an impact load between the ship hull and an isolated ice floe and when the ship encounters ice ridges. Other formulations for the shape dependency, described below, make the same assumption.

Another possibility for shape dependency is given in the proposed ice rules of the International Association for Classification Societies (IACS 2007). In these rules, the ice force is assumed to be proportional to the hull angles as:

$$F \propto \alpha \cdot \beta_n^{-0.5}. \quad (38)$$

A third possibility is to use the relationship (Varsta 1984) that is based on direct calculations of the dynamic bending of ice cover. These results state that the shape proportionality is

$$F \propto \frac{1 + 1.5 \cdot (v_s \cdot \sin \alpha)^{0.4}}{\beta_n - 8.7^\circ}, \beta_n > 15^\circ, [v_s] = \text{m/s}, \quad (39)$$

where v_s is the ship speed. The last formulation for the dependency on hull lines that is considered here is the one used in the 2007 version of the ice rules of the Russian Maritime Register of Shipping (RMRS 2007). Here, the proportionality is given as

$$F \propto 4 \sqrt{\frac{\alpha^2}{\beta}}. \quad (40)$$

These five hull shape proportionality factors are used in the analysis of hull angles. The calculated frame ice force value based on a 1000-day return period in the MT **Kemira** results (bow region) is extrapolated to another vessel using the proportionalities described above ($F = C \cdot f(\alpha, \beta, \varphi)$, C the proportionality factor) as:

$$q_{ship} = \frac{q_{Kemira}}{f(\alpha_{Kemira}, \beta_{Kemira}, \varphi_{Kemira})} \cdot f(\alpha_{ship}, \beta_{ship}, \varphi_{ship}), \quad (41)$$

where the constant C is the hull ice load shape proportionality factor and the line load value is used instead of force. The 1000-day frame force for MT **Kemira** is 2310 kN/m. The results of this analysis are shown in Table 14.

Table 14. Predicted ice load [kN/m] on three ships based on the extrapolation from the MT **Kemira** results. In the method Varsta (1984), the ship speed is taken as 4 m/s.

Method \ Ship	Izumiyama (2005)	Kujala (1994)	IACS (2007)	Varsta (1984)	RMRS (2007)	Measured (1000 days)
IB Sisu	1060	740	1890	800	2050	2290
MV Arcturus	1810	1620	1780	1520	1990	2010
MT Kashira	2520	2630	2540	2730	2370	1780

There is much scatter in shape factors. All give similar results for MV **Arcturus** and MT **Kashira**, but the two rule formulations give much deviation from the other factors for IB **Sisu**. As the calculated force is based on the MT **Kemira** results, it would be surprising if the values obtained for IB **Sisu** were close to the actual measured value, as IB **Sisu** is navigating much more aggressively than MT **Kemira**. Thus, if IB **Sisu** were navigated as MT **Kemira**, the expected forces would be much less than the actual observed value in IB **Sisu** measurements. This gives plausibility to the factors given by Kujala (1994) and Varsta (1984). It is difficult to draw conclusions however.

7.2 Strength Level Validation

The required strength level of the ice class rules – or any structural rules for that matter – is not something exact that can be calculated from the first principles. It depends on how much damage, in a very general sense, is accepted. How close the different limit states are in terms of loading also influences the selection of the required strength level. If there is not much plastic reserve after the yield point, i.e., the load causing collapse is close to the load causing the first yield, then the required strength level must be set quite high. Methods have been developed to evaluate the probability of failure or structural reliability, but all these require knowledge about the ice load statistics and this is only known about in a rudimentary fashion. The only method left to assess the adequate strength level is feedback from past experience.

The feedback from past experience must be collected in an organized fashion. One way to do this is to look at accidents that happen during the winter season compared with other seasons. The number of tanker accidents annually in the Gulf of Finland is shown in Fig. 27, and the accidents that occur during the winter months are shown separately. As the winter season is about four months long, there seems to be a slightly increased risk of accidents during the winter. Unfortunately, the HELCOM database does not allow the investigation if ice cover was the cause of the accident – but judging from the locations of the accidents, ice rarely caused any major accidents. This may be a matter of reporting.

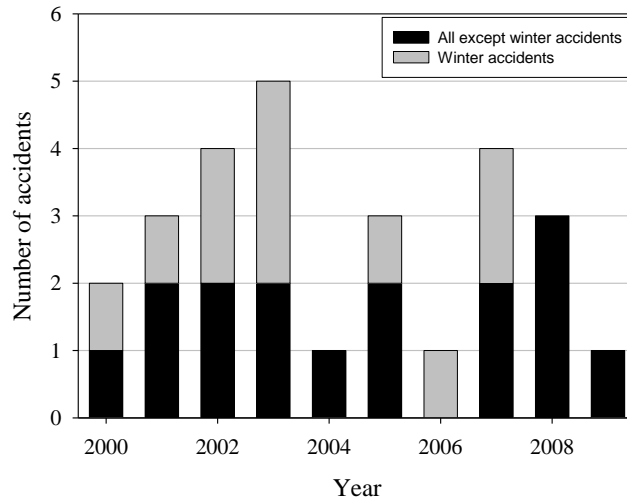


Fig. 27. Tanker accidents in the Gulf of Finland separated into accidents in winter (January to April) and other times; accident data from the HELCOM database (www.helcom.fi)

Three major Baltic ice damage data collections have been carried out: Johansson (1967), Kujala (1991), and Hänninen (2005). The first one of these resulted in the ice class rules of 1971. It also defined the strength level that has basically been followed since, even if several modifications to the loading have been made. The next damage data collection occurred at the end of the 1980s and thus not many ships built under the 1985 FSICRs were included. This damage data collection indicated that longitudinally framed ships are quite susceptible to ice damage – this drawback was corrected in the 1985 rules when the load height was reduced while keeping the ice loading constant.

Finally, the winter 2003 ice damage data collection covered a winter that was more severe than almost ten preceding ones. Quite a large amount of damage of different kinds was observed, with more than 100 cases. Many cases related to practices that had become slacker during the preceding mild winters however. During the winter, 27 cases of hull damage were observed; see Fig. 28. This number represents about 0.2% of all the port calls during the winter. Hull ice damage cannot thus be considered very frequent. This indicates that the strength level of the rules is at an acceptable level.

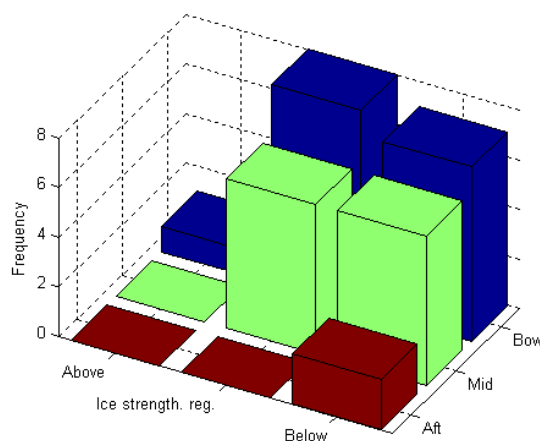


Fig. 28. Amount of hull ice damage observed during winter 2003 (Hänninen 2005)

The final matter to be investigated is the advantage that can be gained by having an ice class. The traffic restrictions to ports in the Gulf of Finland often vary from country to country. For the present winter, the ice class requirement for Russia and Estonia has been the minimum ice class of IC,

whereas to Finnish ports the requirement has been IA. Is there an increased risk of ice damage using lower ice class tonnage?

This question can be answered by looking at the ice damage data from winter 2003, Hänninen (2005); see Fig. 29. These data only include ships bound to and from Finnish ports (100 cases of ice damage, 10,000 port calls with about 1000 different ships). The ice damage data suggest that the majority of ships damaged had an ice class of IA or IA Super (59% of all cases). If the ice damage is calculated per port call, then the probability of ice damage for IA and IA Super ships is 0.7%, whereas the same figure for II and IC ice classes is 6.0%. The probability of ice damage is about nine times greater for low ice class ships: ice class surely has an impact on susceptibility to ice damage.

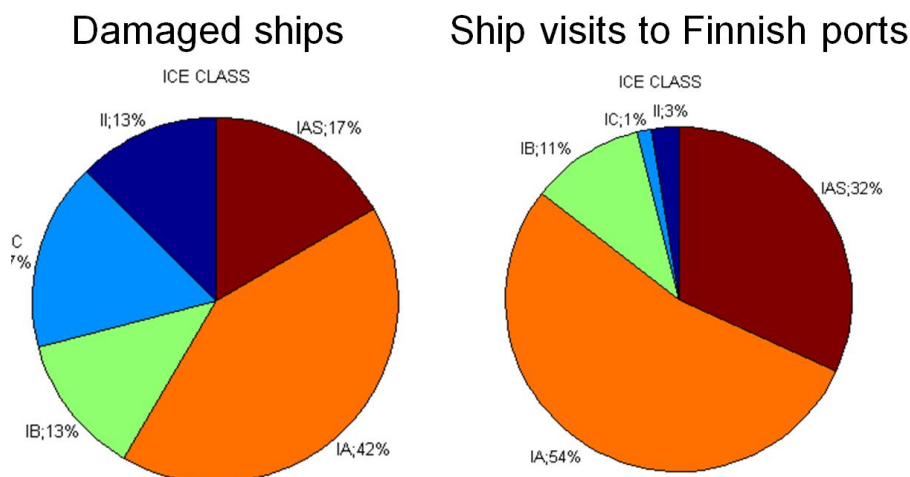


Fig. 29. Amount of ice damage and port calls to Finland separated based on the ice class, Hänninen (2005)

8. CONCLUSION

The Finnish rules for winter navigation have a long history stemming back to 1890 when the first rules were given. These rules, currently called the Finnish-Swedish Ice Class Rules (FSICR), are an integral part of the winter navigation system. Finnish trade is highly dependent on a marine connection, as about 90% of the trade is transported by sea and, as all Finnish ports are ice bound in an average winter, it is clear that winter navigation is crucial to Finland. This situation is less dominant for Sweden, as Sweden has ice-free ports on its west coast.

Winter navigation depends on ice-strengthened merchant ships to navigate efficiently without undue stoppages in traffic, which is often line traffic with fixed schedules. In order to achieve a winter navigation system that runs smoothly, all ships that fulfill the requirements for a minimum amount of cargo and an ice class are given an icebreaker escort to and from the Finnish and Swedish ports. Furthermore, the safety of shipping is ensured by an adequate strength level given in the ice class rules, and the need for icebreakers is optimized by requiring some minimum ice-going performance from merchant ships in the ice class rules.

Winter navigation – or rather year-round navigation – is considered to have started when the steamer **SS Express II** sailed on her maiden voyage on 12/15/1877 from the Finnish port of Hanko to Stockholm in Sweden. Since those days, winter navigation has expanded, and since the late 1960s all Finnish and Swedish ports have been kept open. In 1966, Finland and Sweden agreed to develop the winter navigation system together – this resulted in, among other things, the first

Finnish-Swedish Ice Class Rules in 1971 and an order for an icebreaker series, the Urho class. Three of these icebreakers were built for Sweden and two for Finland.

The 1971 ice class rules were based on an extensive ice damage survey and resulted in the required strength level for the hull and machinery being established. These strength levels (each ice class has its own strength level) have essentially remained unaltered since then. The 1971 ice class rules also defined the ice load explicitly for the first time. Although the rules have seen several changes, the rule structure is similar, even in the newest 2010 rules. Experiences of ships built for the Finnish-Swedish ice classes have made several changes necessary to the rules since 1971. In 1985, the new knowledge about ice loads was incorporated into the rules and, at the same time, the strength level for longitudinally framed ships was made adequate. In 1999 and, slightly modified, in 2002, the new requirements for ice-going performance were given. The machinery rules were amended in 2008 and, finally, in 2010, the hull rules were streamlined to remove any inconsistencies that had remained in the load and strength definitions.

The Finnish-Swedish Ice Class Rules can be considered very robust, as every winter about 10,000 ship visits test the rule strength and ice performance levels. The present winter (2011) has been a little more severe than the long-term average. Some rudder and propeller damage has been observed, but the feeling is that the amount of ice damage is not alarmingly high. The ice performance of ships, on the other hand, is an issue that has to be investigated, as the traffic to the northernmost ports in Finland and Sweden ran very slowly for several weeks in winter 2011. Shipowners claim that they have lost several hundred ship-days in delays. Again, feedback from the existing winter navigation system may give an initiative for changes. This quick accommodation of the ice class rules to the 'facts of life' is the strength of the Finnish-Swedish Ice Class Rules.

REFERENCES

- Daley, C. 2002a: Derivation of Plastic Framing Requirements for Polar Ships. *Marine Structures*, Vol. 15, pp. 544-559.
- Daley, C. 2002b: Application of Plastic Framing Requirements for Polar Ships. *Structures*, Vol. 15, pp. 533-542.
- Frederking, R. & Sudom, D. 2008: Local Ice Pressure Distributions during 1990 Hobson's Choice Ice Island Multi-Year Ice Indentation Tests. *Proc. 19th IAHR Symposium on Ice*, Vol. 2, pp. 815-827, Vancouver, B.C. Canada, 2008.
- Frederking, R. & Kubat, I. 2005: Definition and Application of Pressure-area Relations and Line Load Distributions. Deliverable D3-2 from the project SAFEICE. In Kujala, ed. (2007), Vol. 1, pp. 134-150.
- Gyldén, R. & Riska, K. 1989: Ice Load Measurements onboard the MS Kemira, Winter 1990. Helsinki University of Technology, Laboratory of Naval Architecture and Marine Engineering, Report M-93, 13 p. + app.
- Hayward, R. 2001: Plastic Response of Ship Shell Plating Subjected to Loads of Finite Height. ME thesis, Faculty of Engineering and Applied Science, Memorial University of Newfoundland, Canada, 113 p. + app.
- Hayward, R. 2007: Principles of Plastic Design. Report D8-4 from the SAFEICE project, 21 p. (see also Kujala, ed. 2007).
- Holtmark, G. & Strömme, H. 2004: The Capacity of Panel Stiffeners Subjected to Lateral Pressure Loads. Det Norske Veritas, Technical Report No. 2004-0168, 39 p.

- Hänninen, S. 2002: The Use of Statistical Methods in Determination of Design Ice Load on Ship Hull Frame in the Baltic Sea [in Finnish]. M.Sc. thesis, Helsinki University of Technology, Department of Mechanical Engineering, 100 p. + app.
- Hänninen, S. 2005: Incidents and Accidents in Winter Navigation in the Baltic Sea, Winter 2002-2003. Winter Navigation Research Board, Research Report No. 54, Helsinki, 39 p.
- IACS 2007: Requirements Concerning Polar Class. International Association of Classification Societies, 38 p.
- Izumiyama, K. 2005: Description of Local Ice Loading and Hull Area Factors based on Model Test Results. Deliverable D3-1 from the SAFEICE project. In Kujala, ed. (2007), Vol. 1, pp. 115-133.
- Johansson, B. 1967: On the Ice Strengthening of Ship Hulls. International Ship Building Progress, vol. 14, pp. 231-245.
- Kaldasau, J. 2010: Risk-Based Approach for Structural Design of Ice-Strengthened Vessels Navigating in the Baltic Sea. M.Sc. thesis, Aalto University School of Science and Technology, Department of Applied Mechanics, 83 p. + app.
- Kujala, P. & Vuorio, J. 1986: Results and Statistical analysis of Ice Load Measurements on Board Icebreaker **Sisu** in Winters 1979 to 1985. Winter Navigation Research Board, Research Report No 43, Helsinki. 52 p. + app. 73 p.
- Kujala, P. 1989: Results of Long-Term Ice Load Measurements onboard Chemical Tanker **Kemira** in the Baltic Sea during the Winters 1985 to 1988. Winter Navigation Research Board, Research Report No. 47, 55 p. + app.
- Kujala, P. 1991: Damage Statistics of Ice-Strengthened Ships in the Baltic Sea. Winter Navigation Research Board, Research Report No. 50, Helsinki, 66 p.
- Kujala, P. 1994: On the Statistics of Ice Loads on Ship Hull in the Baltic. Acta Polytechnica Scandinavica, Mechanical Engineering Series No. Me 116, 98 p.
- Kujala, P. ed. 2007: Increasing the Safety of Icebound Shipping, Final Scientific Report, Vol. 2. Helsinki University of Technology, Ship Laboratory, Report M-302, 347 p.
- Lensu, M. 2002: Short Term Prediction of Ice Loads Experienced by Ice Going Ships. Helsinki University of Technology, Ship Laboratory, Report M-269, 59 p.
- Lindholm, J-E., Riska, K., & Joensuu, A. 1990: Contact between Structure and Ice – Results from Ice Crushing Tests with Flexible Indentor. Helsinki University of Technology, Laboratory of Naval Architecture and Marine Engineering, Report M-101, Otaniemi, 30 p. + app.
- Muhonen, A. 1991: Ice Load Measurements onboard the MS Kemira, Winter 1990. Helsinki University of Technology, Laboratory of Naval Architecture and Marine Engineering, Rpt M-109, 24 p. + app.
- Muhonen, A. 1992: Ice Load Measurements onboard the MS Kemira, Winter 1991. Helsinki University of Technology, Laboratory of Naval Architecture and Marine Engineering, Rpt M-121, 26 p. + app.
- NORSOK Standard N-004 2004: Design of Steel Structures. Standards Norway, 287 p.
- Ranki, E. 1986: Determination of Ice Loads from the Permanent Deformations of Shell Structure in Ships [in Finnish]. Lic. Tech. thesis, Helsinki University of Technology.
- Riska, K., Rantala, H., & Joensuu, A. 1990. Full Scale Observations of Ship-Ice Contact. Helsinki University of Technology, Lab. of Naval Architecture and Marine Eng., Report M-97, Espoo, 1990, 54 p. + 293 app.
- Riska, K. & Windeler, M. 1997: Ice-Induced Stresses in the Shell Plating of Ice-Going Vessels. Helsinki University of Technology, Arctic Offshore Research Centre, Rpt M-219, Otaniemi, Finland, 34 p.
- Riska, K., Uto, S., & Tuhkuri, J. 2002: Pressure Distribution and Response of Multiplate Panels

- under Ice Loading. *Cold Regions Science and Technology*, 34(2002), pp. 209-225.
- Riska, K. 2006a: Factors Influencing the Power Requirement in the Finnish-Swedish Ice Class Rules. Report to the Finnish Maritime Administration, to be published in the Winter Navigation Research Board report series, 63 p.
- Riska, K. 2006b: Ice Classification of Large Vessels. Conference on the Winter Navigation on the Baltic Sea, ICEDAY 2006, 9-10 February, 2006, Kemi.
- Riska, K. 2007: Application of the SAFEICE Project Results in Developing the Finnish Swedish Ice Class Rules. Deliverable D7-3 from the SAFEICE project. In Kujala, ed (2007), 27 p.
- Riska, K. 2011: Design Point in Ice Class Rules. Report to the Finnish Transport Safety Agency, to be published in Winter Navigation Research Board report series, 34 p.
- RMRS 2007: Rules for the Classification and Construction of Sea-Going Ships. Russian Maritime Register of Shipping, Vol. 1, Saint Petersburg, 461 p.
- Siivonen, O. 1977: The Development of Finnish Ice Class Rules. Ice, Ships and Winter Navigation Symposium, Oulu 16-17.12.1977, pp. 154-171.
- Sodhi, D, Takeuchi, T., Nakazawa, N., Akagawa, S., & Saeki, H. 1998: Medium-scale indentation tests on sea ice at various speeds. *Cold Regions Science and Technology*, Vol. 28, pp. 161-182.
- Su, B., Riska, K., & Moan, T. 2010: Numerical Simulation of Local Ice Loads in Uniform and Randomly Varying Ice Conditions. *Cold Regions Science and Technology*, Vol. 65, pp. 145-159.
- Trafi 2010: Ice Class Regulations 2010: "Finnish-Swedish Ice Class Rules 2010." Finnish Transport Safety Agency, 23.11.2010 TRAFI/31298/03.04.01/2010, 48 p.
- Tuhkuri, J. 1993: Laboratory Tests of Ship Structures under Ice Loading, Vol. 1. Helsinki University of Technology, Ship Laboratory, Report M-166, Otaniemi, 171 p.
- Uto, S. 2000: Influence of Plate Rigidity on Ice Loading under Line-Like Contact between Ice and Stiffened Ship Hull Structure. Report M-254, Arctic Offshore Research Centre, Helsinki University of Technology, 47 p.
- Valanto, P. 2005: Spatial Distribution of Numerically Predicted Ice Loads on Ship Hulls in Level Ice. Deliverable D6-3 from the project SAFEICE. In Kujala, ed. (2007), Vol. 2, pp. 25-51.
- Valkonen, J. 2006: Determination of Ship Ice Load from Hull Ice Damages. M. Sc. thesis, Helsinki University of Technology, Ship Laboratory, 98 p. + app.
- Varsta, P., Droumev, I. & Hakala, M. 1978: On Plastic Design of an Ice-Strengthened Frame. Winter Navigation Research Board, Report No. 27, 54 p.
- Varsta, P. 1983: On the Mechanics of Ice Load on Ships in Level Ice in the Baltic Sea. Technical Research Centre of Finland, Publication No. 11, 91 p.
- Varsta, P. 1984. Determination of Ice Loads Semi-empirically. Ship Strength and Winter Navigation, VTT Symposium 52, pp. 177-182.
- Vuorio, J., Riska, K., & Varsta, P. 1979: Long-Term Measurements of Ice Pressure and Ice-Induced Stresses on the Icebreaker **SISU** in Winter 1978. Winter Navigation Research Board, Research Report no. 28, 50 p.

Corresponding author: Kaj Riska
 E-mail: kajrisk@welho.com (or kaj.riska@ils.fi)
 Address: Lökkikuja 5E
 00200 Helsinki, FINLAND